Phase field models for step flow

O. Pierre-Louis
LSP-Grephe, CNRS/UJF, Grenoble 1, Boîte Postale 87, F-38042 Saint Martin d'Hères Cedex, France
(Received 24 January 2003; published 15 August 2003)

The relation between phase field and discontinuous models for crystal steps is analyzed. Different formulations of the kinetic boundary conditions of the discontinuous model are first presented. We show that (i) step transparency, usually interpreted as the possibility for adatoms to jump through steps, may be seen as a modification of the equilibrium concentration engendered by step motion. (ii) The interface definition (i.e., the position of the dividing line) intervenes in the expression of the kinetic coefficients only in the case of fast attachment kinetics. (iii) We also identify the thermodynamically consistent reference state for kinetic boundary conditions. Asymptotic expansions of the phase field models in the limit where the interface width is small, lead to various discontinuous models. (1) A phase field model with one global concentration field and variable mobility is shown to lead to a discontinuous model with fast step kinetics. (2) A phase field model with one concentration field per terrace allows one to recover arbitrary step kinetics (i.e., arbitrarily strong Ehrlich-Schwoebel effect and step transparency). Quantitative agreement is found, in both the linear and nonlinear regimes, between the numerical solution of the phase field models and the analytical solution of the discontinuous model.

DOI: 10.1103/PhysRevE.68.021604 PACS number(s): 81.10.Aj, 81.15.Hi, 68.35.Ct

I. INTRODUCTION

From molecular dynamics to the macroscopic continuum, the description of a crystal surface may take a wide variety of forms, depending on the range of scales that is used. As a mesoscopic approach at intermediate scales, modeling the surface as a collection of crystal steps separated by high symmetry terraces is a powerful tool for studying surface statics and dynamics [1].

Progress in the understanding of nonequilibrium surface dynamics has been achieved. Still, many questions remain open such as the precise link between microscopic atom motion and step kinetics [2], steps dynamics out of the weakly unstable regimes [3,4], or in complex geometries [5,6]. Steps dynamics is nonlinear and nonlocal in time and space—as can be seen explicitly by means of a Green's function formalism [7,8]. Nonlocality comes from the coupling of steps via the diffusion of adatoms on terraces. Nonlinearities arise from step geometry, but also from the fact that steps are free moving boundaries.

In the phase field approach, the interface (the step) is a region of fast but continuous variation of an order parameter (or phase field). Phase field models can be seen as an intermediate description between molecular dynamics and steps dynamics, opening new ways for a quantitative link through the length scales. Since they do not require an explicit tracking of the fronts, phase field models also simplify the numerical computation of steps dynamics.

Several studies were already devoted to the phase field formulation of steps dynamics [6,7]. In this paper, we focus on a comprehensive and quantitative description of step kinetics.

We first present a discontinuous model for steps with general kinetics. Some discussion and rewriting of the boundary conditions are presented. These alternative formulations contain some interesting hints about the physical interpretation of step kinetics.

(i) The microscopic origin of step transparency is discussed. It is found that transparency, traditionally related to motion of mobile atoms through steps [9,10], can be seen as a modification of the equilibrium concentration engendered by step motion. This allows an explicit link with the kinetic boundary conditions used in solidification [11].

(ii) The interface definition (i.e., the arbitrary position of the dividing line which allows to calculate interface excess quantities) intervenes in the expression of the kinetic coefficients only in the case of fast attachment kinetics. But the model is still well defined in this limit as opposed to previous work in the literature [12].

(iii) Using the correspondence to phase field models, we identify the reference state for the boundary conditions which is consistent with thermodynamics.

For the first time to the best of our knowledge, the step velocity and the linear dispersion relation for a vicinal surface are calculated from the discontinuous model in the nonquasistatic case with general step kinetics and in the presence of adatom deposition and desorption, including both step meandering and step bunching.

We then present two phase field models. Within different types of asymptotics, the phase field models are shown to lead to different discontinuous models. Despite the lengthy algebra of the asymptotic expansions, an overall simple physical picture arises that connects the length scales.

A phase field model with one concentration field is first presented in Sec. III. The so-called *sharp* [13] and *thin* [14] *interface asymptotics* are performed. They lead to discontinuous models with strong transparency and fast attachment kinetics, respectively. The numerical solution of the two-dimensional (2D) phase field model is shown to be in quantitative agreement with the discontinuous model.

Nevertheless, this phase field model cannot account for slow kinetics that may lead to a finite concentration jump at the step (e.g., strong Ehrlich-Schwoebel effect observed on metal surfaces [15] leads to a finite jump of the concentration

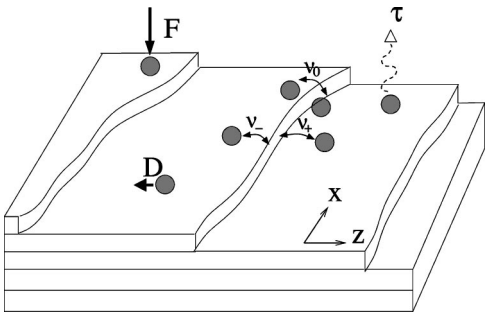

FIG. 1. A vicinal surface with microscopic transport processes.

at the step during growth). In order to solve this problem, we propose a model with one concentration field on each terrace in Sec. VI. This model allows a finite concentration jump at the step. The sharp interface asymptotics is shown to lead to a step model with arbitrary (i.e., not necessarily fast) step kinetics. The numerical solution of the 2D phase field model is in quantitative agreement with the analytical solution of the discontinuous model on at least five orders of magnitude of variation of the kinetic coefficients.

Finally, the nonlinear dynamics of an isolated step during growth is studied. The numerical result of the phase field model is in agreement with the multiscale analysis of the discontinuous model [3].

II. DISCONTINUOUS MODEL

A. Model equations

In the *discontinuous model*, steps are lines that define the boundary of three phases: a solid phase, and two gaseous two-dimensional adatom phases on the neighboring terraces, one behind and one in front of the step. On a terrace, mass conservation is written as an evolution equation for the adatom concentration c:

$$\partial_t c = D\boldsymbol{\nabla}^2 c + F - c/\tau, \tag{1}$$

where ∂_t indicates the derivative with respect to time. As shown in Fig. 1, F is the rate at which atoms are adsorbed on terraces [from a molecular beam or a three-dimensional (3D) gas phase]. D is the diffusion constant of adatoms on terraces and τ is the adatom desorption time. At a step, there are two independent thermodynamic forces:

$$X_\pm = c_\pm - c_{eq}^*, \tag{2}$$

where $\pm$ refers to the diffusion fields in front of and behind the step. The local equilibrium concentration c_{eq}^* depends on the free energy of the steps $\mathcal{F}$. Using a linear thermodynamics picture (linearized Gibbs-Thomson relation), we have, in the vicinity of a step of meander ζ,

$$c_{eq}^* = c_{eq}\left(1 + \frac{\Omega}{k_B T}\frac{\delta \mathcal{F}}{\delta \zeta}\right), \tag{3}$$

where c_{eq}^0 is the equilibrium concentration in the vicinity of a straight step. Here $\mathcal{F}=\int ds\,\gamma$ is the free energy of the step, where s is the step arclength and γ is the line tension. Then one has $(\delta\mathcal{F}/\delta\zeta)=\tilde{\gamma}\kappa$, where κ is the step curvature and $\tilde{\gamma}=\gamma+\gamma''$ is the step stiffness. We then define $\Gamma = \Omega\tilde{\gamma}/k_B T$ such that

$$c_{eq}^* = c_{eq}(1+\Gamma\kappa). \tag{4}$$

There are three mass fluxes at the step: the diffusion fluxes $J_\pm$ and the quantity of matter transformed from 2D gas to solid denoted by J_s,

$$J_\pm = -(D\partial_n c_\pm + V c_\pm), \tag{5}$$

$$J_s = \frac{1}{\Omega}V, \tag{6}$$

where V is the normal step velocity, $1/\Omega$ is the solid concentration, and $\partial_n = \mathbf{n}\cdot\boldsymbol{\nabla}$ is the derivative in the direction normal to the step. They are related through global mass conservation at the step, which is written as $J_s + J_- = J_+$, or

$$\frac{1}{\Omega}V = (-D\partial_n c_- - V c_-) + (D\partial_n c_+ + V c_+). \tag{7}$$

Thus, only two of the three fluxes are independent, and should be related to the thermodynamic forces using linear phenomenological laws. The kinetic boundary conditions are then written as

$$\begin{aligned} -(J_+ - J_r) &= L_{++}X_+ + L_{+-}X_-, \\ (J_- - J_r) &= L_{--}X_- + L_{-+}X_+. \end{aligned} \tag{8}$$

The second term on the left hand side (lhs) is the flux in the reference state for a referential moving at a velocity V:

$$J_r = V c_{eq}\chi. \tag{9}$$

Two cases are considered: adatom vacuum (or bare terrace) reference state $\chi=0$ and equilibrium reference state $\chi=1$. From the link to the phase field models, we will argue in the following that $\chi=1$ is the only thermodynamically consistent model. From Onsager reciprocity relations $L_{-+}=L_{+-} \equiv -\nu_0$. We then define $\nu_+ \equiv L_{++} - \nu_0$ and $\nu_- \equiv L_{--} - \nu_0$. Relations (8) are now written as

$$\begin{aligned} -(J_+ - J_r) &= \nu_+(c_+ - c_{eq}^*) + \nu_0(c_+ - c_-), \\ (J_- - J_r) &= \nu_-(c_- - c_{eq}^*) + \nu_0(c_- - c_+), \end{aligned} \tag{10}$$

$\nu_\pm$ are related to mass exchange between $+$ and $-$ adatom phases and the solid. ν_0 was introduced first in Ref. [10], and describes ''direct'' exchange between terraces, this phenomena is called step transparency. The different kinetic processes at the step are depicted in Fig. 1. One then has

$$\frac{V}{\Omega} = \nu_+(c_+ - c_{eq}^*) + \nu_-(c - c_{eq}^*). \tag{11}$$

Interestingly, this relation shows that the term $Vc_\pm - Vc_{eq}\chi$ on the lhs of Eq. (10) is second order in the departure from

equilibrium $(c-c_{eq}^{*})$ when $\chi=1$. Similarly, the term $V(c_+ - c_-)\sim(c-c_{eq})^2$ on the right-hand side (rhs) of Eq. (7). In a linearized picture, these terms can be neglected, and $J - J_r \approx -D\partial_n c$.

B. Discussion of the boundary conditions

1. Step transparency and link to solidification

Equations (1), (7), and (10) [with Eq. (3)] describe the deterministic dynamics of a set of steps as long as step nucleation or collision does not occur. This formulation allows one to interpret ν_0 as a kinetic coefficient for mass exchange between terraces. But linear combinations of Eqs. (7) and (10) lead to alternative and equivalent sets of boundary conditions. As a first example, kinetic laws at the step may also be written as

$$-(J_+ - J_r) = \tilde{\nu}_+ (c_+ - \tilde{c}_{eq}),$$

$$(J_- - J_r) = \tilde{\nu}_- (c_- - \tilde{c}_{eq}), \tag{12}$$

where we have defined

$$\tilde{c}_{eq} = c_{eq}(1+\Gamma\kappa) + \tilde{\beta}\frac{V}{\Omega}, \tag{13}$$

and the kinetic coefficients

$$\tilde{\nu}_+ = \nu_+ + \nu_0(1+\nu_+/\nu_-), \tag{14}$$

$$\tilde{\nu}_- = \nu_- + \nu_0(1+\nu_-/\nu_+), \tag{15}$$

$$\tilde{\beta} = \left(\frac{\nu_+\nu_-}{\nu_0} + \nu_+ + \nu_-\right)^{-1}. \tag{16}$$

In the limit of opaque steps ($\nu_0 \to 0$), Eqs. (10) and (12) are identical. Equation (12) shows that step transparency ($\nu_0 \neq 0$), usually described as the possibility for direct exchange of atoms between terraces, can equivalently be seen as a correction of the equilibrium concentration at the step due to step motion [term $\tilde{\beta}V$ in Eq. (13)]. In the limit $\nu_0 \to \infty$, we recover boundary conditions similar to that used in solidification [16] (here, concentration replaces temperature):

$$c_+ = c_- = c_{eq}(1+\Gamma\kappa) + \tilde{\beta}\frac{V}{\Omega}. \tag{17}$$

Note that the attachment-detachment asymmetry (Ehrlich-Schwoebel effect) is irrelevant in this limit.

2. Global-exchange boundary conditions

A third equivalent formulation will naturally appear in Sec. IV from the analysis of the phase field model. The first two equations account for global mass conservation at each side of the step:

$$-(J_+ - J_r) = \alpha\frac{V}{\Omega} + \nu(c_+ - c_-),$$

$$(J_- - J_r) = (1-\alpha)\frac{V}{\Omega} + \nu(c_- - c_+), \tag{18}$$

where α measures the kinetic asymmetry of the step. ν is the global-exchange kinetic coefficient between terraces, naturally arises from the solution of the discontinuous model (see Appendix E and Ref. [17]). A third equation, equivalent to Eq. (11), relates the velocity to an asymmetric thermodynamic force:

$$\frac{V}{\Omega} = \frac{1}{\beta}[\alpha(c_+ - c_{eq}^{*}) + (1-\alpha)(c_- - c_{eq}^{*})], \tag{19}$$

where β is a kinetic coefficient having the dimension of the inverse of a velocity. The new kinetic coefficients can be related to the previous ones via

$$\nu = \nu_0 + (\nu_+^{-1} + \nu_-^{-1})^{-1}, \tag{20}$$

$$\alpha = \frac{\nu_+}{\nu_+ + \nu_-}, \tag{21}$$

$$\beta = \frac{1}{\nu_+ + \nu_-}. \tag{22}$$

C. Step dynamics on a vicinal surface

A vicinal surface is a (staircaselike) surface where all steps have the same orientation. During growth or sublimation, there exists a steady state for a vicinal surface with equidistant and straight steps, where all steps have the same velocity. This is the step flow growth mode. Since it is free of nucleation events, this growth mode is a candidate for the production of atomically flat surfaces in molecular beam epitaxy. Using Eqs. (1), (7), and (10), the steady state concentration and the step velocity were extracted.

In the quasistatic limit, which is widely used in the literature, the lhs of Eq. (1) is neglected. Moreover, it is supposed that $Vc \ll D|\nabla c|$, so that the diffusion flux is $J \approx -D\nabla c$. This approximation is not justified when diffusion is slow (e.g., at low temperature or for large molecules) or when the concentration is high. An implicit expression for the full nonquasistatic step velocity is given in Appendix E.

During growth, a meandering instability appears in the presence of a normal Ehrlich-Schwoebel effect, $\nu_+ > \nu_-$ and a bunching instability in the presence of an inverted Ehrlich-Schwoebel effect; $\nu_+ < \nu_-$. These kinetic instabilities may be considered as a source of undesired surface roughness. On the other hand, this spontaneous pattern formation may be used to produce large scale networks of nanostructures. The reader interested in an extended discussion of the stability of a vicinal surface should refer to the literature [18,19]. The nonquasistatic linear stability analysis of the model was performed and the dispersion relation is written in Appendix E. From this implicit relation, the rate of amplification or decay of a small perturbation is extracted numerically.

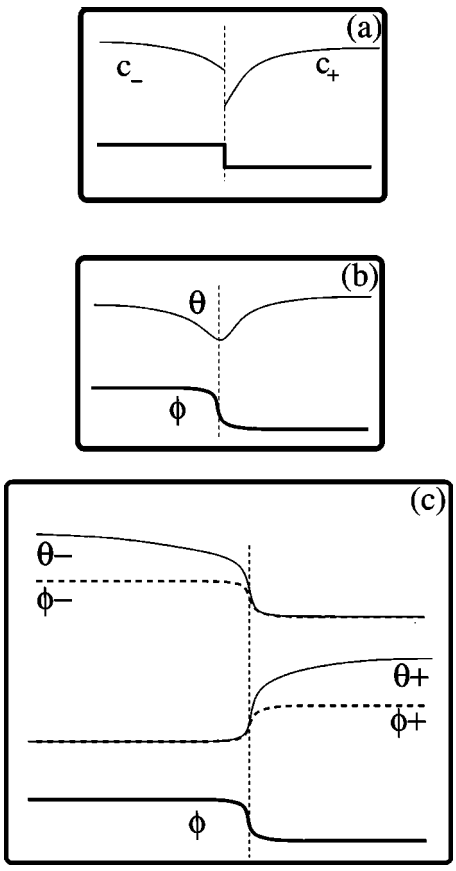

FIG. 2. Discontinuous model (a). Phase field model with one concentration field (b) and with one concentration field per terrace (c). (Although this schematic is one-dimensional and with only one step, all models are two-dimensional and the number of steps is arbitrary.)

When steps are morphologically unstable, a multiscale analysis must be performed in order to predict nonlinear dynamics at long times. As an example, in the case of an isolated step, Bena *et al.* [3] have shown that the meander obeys the Kuramoto-Sivashinsky equation, which exhibits spatiotemporal chaos.

In the following, we will use these analytical predictions of the discontinuous model (i.e., step velocities, meandering and bunching rates, and nonlinear dynamics) in order to check the quantitative agreement between the discontinuous and phase fields models.

III. PHASE FIELD COUPLED TO ONE GLOBAL CONCENTRATION FIELD

A. Model

The traditional phase field model is a model with a phase field ϕ coupled to a driving field. In the limit where the width of the interface is small, different discontinuous models have been obtained, depending on the precise asymptotics that is used [13]. Some phase field models for steps were already proposed [6,7].

In this section, we present an extended version of the phase field model with one concentration field depicted in Fig. 2, which includes a variable mobility of the atoms in the step region.

The first model equation accounts for the evolution of the adatom coverage $\theta=\Omega c$ (where Ω is the atomic area):

$$\partial_t \theta = \boldsymbol{\nabla}[M \boldsymbol{\nabla} \theta] + \Omega F - \frac{\theta}{\tau} - \partial_t h, \tag{23}$$

where M is the nonconstant adatom diffusion constant and h, the solid concentration, is defined up to an additive constant. The second equation is an evolution equation for the phase field ϕ itself:

$$\tau_p \, \partial_t \phi = W^2 \nabla^2 \phi - f_\phi + \lambda(\theta - \theta_{eq}) g_\phi, \tag{24}$$

where W is the interface width. M, h, f, and g are periodic functions of ϕ. The index ϕ indicates derivation with respect to ϕ. f is an energy density having minima for values of ϕ corresponding to terraces. g is a coupling function defined in such a way that g_ϕ and $g_{\phi\phi}$ both vanish at the minima of f. This model can be further generalized to account for a nonconstant equilibrium concentration. Nevertheless, this modification does not affect the main conclusions of the present section, as shown in Appendix A.

In the following, the thin and the sharp interface asymptotics will be presented. In both limits, the product $\lambda(\theta - \theta_{eq})$ is small. In the sharp interface asymptotics, the coupling constant λ is small. This corresponds to a weak coupling limit, i.e., steps are very transparent. In the thin interface limit, the coupling constant is not small, but the departure from equilibrium at the interface $\theta - \theta_{eq}$ is small. This means that we assume that interface kinetics is fast enough for θ to relax to a value which is near θ_{eq}. In the following, we describe both types of asymptotics in more detail.

B. Thin interface limit

1. Expansion

Starting from a phase field model with constant mobility $M=D$, Karma and Rappel [14] have presented a form of asymptotics, called the thin interface limit, that accounts for step dynamics with instantaneous attachment kinetics.

In order to extract an effective discontinuous model from the phase field model with variable mobility (23) and (24), an asymptotic expansion is performed, following the lines of the thin interface limit presented in Ref. [14]. Let us define the small parameter $\epsilon = W/\ell_c$, where ℓ_c is a cutoff length related to diffusion on terraces. In the following, all distances are normalized by ℓ_c, so that $\epsilon = W$. We expect the field ϕ to stay in minima of the free energy f in wide areas, which define terraces. From one terrace to another, ϕ smoothly jumps from one minima to the other. Thus, two regions are considered, where two different expansions are made. An inner region (the step region), where the fields have zeroth-order variations on a distance of order W. An outer region (terraces), where the fields might have zeroth-order variations on a distance of order ℓ_c. The geometry of the inner region is imposed by the position of the step, where normal and arclength variables r and s are defined. In the inner region, we define the variable $\eta = r/W$ and the inner fields

$\theta^{in}(\eta,s)$ and $\phi^{in}(\eta,s)$. These fields are expanded as

$$\theta^{in}(\eta,s)=\theta_0^{in}(\eta,s)+W\theta_1^{in}(\eta,s)+W^2\theta_2^{in}(\eta,s)+\cdots, \tag{25}$$

$$\phi^{in}(\eta,s)=\phi_0^{in}(\eta,s)+W\phi_1^{in}(\eta,s)+W^2\phi_2^{in}(\eta,s)+\cdots. \tag{26}$$

Model equations (23) and (24) are expanded up to first order in W in the inner region

$$o(W^2)=\partial_\eta[M\,\partial_\eta\theta^{in}]+W(V+M\kappa)\partial_\eta\theta^{in}+WV\,\partial_\eta h, \tag{27}$$

$$o(W^2)=\partial_{\eta\eta}\phi^{in}-f_\phi+\lambda(\theta^{in}-\theta_{eq})g_\phi+W(Va+\kappa)\partial_\eta\phi^{in}, \tag{28}$$

where κ is the curvature of the step. The step diffusion constant

$$\frac{1}{a}=\frac{W^2}{\tau_\phi} \tag{29}$$

is taken to be $\sim o(1)$, hence $\tau_\phi\sim W^2$. This choice ensures that the internal dynamics of the step is fast enough to maintain a well defined step in nonequilibrium situations.

In the outer region, far from steps, the phase field ϕ lies in a (stable) minima of the energy density f. The coverage θ^{out} then obeys

$$\partial_t\theta^{out}=D\nabla^2\theta^{out}+\Omega F-\frac{\theta^{out}}{\tau}, \tag{30}$$

which is equivalent to Eq. (1). In the vicinity of a step, the outer field is expanded as

$$\theta^{out}(\eta,s)=\theta_0^{out}(\eta,s)+W\theta_1^{out}(\eta,s)+W^2\theta_2^{out}(\eta,s)+\cdots, \tag{31}$$

$$\phi^{out}(\eta,s)=\phi_0^{out}(\eta,s)+W\phi_1^{out}(\eta,s)+W^2\phi_2^{out}(\eta,s)+\cdots. \tag{32}$$

Matching of the inner expansion at $\eta\to\infty$ with the outer expansion at $r\to 0$ leads to the following conditions:

$$\lim_{\eta\to\pm\infty}\theta_0^{in}=\theta_{0\pm}^{out}, \tag{33}$$

$$\lim_{\eta\to\pm\infty}\partial_\eta\theta_0^{in}=0, \tag{34}$$

$$\lim_{\eta\to\pm\infty}\theta_1^{in}=\theta_{1\pm}^{out}+(\eta-\overline{\eta})\partial_r\theta_{0\pm}^{out}, \tag{35}$$

$$\lim_{\eta\to\pm\infty}\partial_\eta\theta_1^{in}=\partial_r\theta_{0\pm}^{out}, \tag{36}$$

$$\lim_{\eta\to\pm\infty}\partial_{\eta\eta}\theta_1^{in}=0, \tag{37}$$

where the index $\pm$ on the rhs indicates that the limit $\lim_{r\to 0\pm}$ was taken. $\overline{\eta}$ is an arbitrary constant which defines the position of the interface to first order. We have written only the relations that will be needed. Similar matching relations hold for ϕ. The reader should refer to Ref. [13] for a derivation of the above matching conditions.

2. Zeroth order

The index in will be omitted in the following. To leading order, Eq. (27) reads

$$\partial_\eta[M^0\,\partial_\eta\theta_0]=0. \tag{38}$$

Integrating this equation, one gets $M_0\,\partial_\eta\theta_0=A_0$ a constant. From the matching condition (34), we must have $A_0=0$. As a consequence, $\theta_0=\overline{\theta_0}$ is a constant. To this order, the evolution equation of the phase field Eq. (24) leads to

$$\partial_{\eta\eta}\phi_0-f_\phi^0+\lambda(\overline{\theta_0}-\theta_{eq})g_\phi^0=0, \tag{39}$$

where f^0 means f evaluated at $\phi=\phi_0$. Equation (39) is easily solved using an analogy with point mechanics in a one-dimensional potential. ϕ and η correspond to position and time, respectively. The particle of unit mass moves in the potential $-f+\lambda(\overline{\theta_0}-\theta_{eq})g$. It has to go from a maxima of the potential to the other, with vanishing initial and final velocities to agree with the matching conditions (34). If we choose g such that

$$g_+^0-g_-^0=[g^0]_-^+\neq 0, \tag{40}$$

the only solution is $\overline{\theta_0}=\theta_{eq}$ (for which the maxima have the same height), and

$$\partial_{\eta\eta}\phi_0-f_\phi^0=0. \tag{41}$$

This equation has localized "kink solutions" ϕ_0, going from one minima of f to the next one. The width of this kink is ~ 1 in η coordinate, which corresponds to a width W in physical coordinates. By definition, these kinks are the steps.

3. First order

The subdominant contribution in the diffusion equation, Eq. (27), reads

$$\partial_\eta[M^0\,\partial_\eta\theta_1]+V\,\partial_\eta\phi_0\,h_\phi^0=0, \tag{42}$$

which leads, after two integrations[1] with respect to η, to

$$\theta_1=-V\int_0^\eta d\eta'\frac{h^0}{M^0}+A_1\int_0^\eta d\eta'\frac{1}{M^0}+B_1, \tag{43}$$

where A_1 and B_1 are constants. Since $\lim_{\eta\to+\infty}\partial_{\eta\eta}\theta_1=0$, taking the limit $\eta\to\infty$ in Eq. (43) leads to

$$\lim_{\eta\to+\infty}\theta_1=Y_{1+}+\eta Z_{1+}, \tag{44}$$

[1]Matching after only one integration is sufficient to derive mass conservation, but for the sake of clarity, the complete matching is postponed to later in the derivation.

where Y_{1+} and Z_{1+} are constants that depend on A_1 and B_1. From the matching conditions, Eq. (35), we have $Y_{1+} = \theta_{1+}^{out} - \overline{\eta}\,\partial_r \theta_{0+}^{out}$ and $Z_{1+} = \partial_r \theta_{0+}^{out}$. Similar relations may be written on the $-$ side: $Y_{1-} = \theta_{1-}^{out} - \overline{\eta}\,\partial_r \theta_{0-}^{out}$ and $Z_{1-} = \partial_r \theta_{0-}^{out}$. Thus, we have four relations.

On the other hand, Eq. (28) to first order reads

$$\partial_{\eta\eta}\phi_1 - \phi_1 f_{\phi\phi}^0 = -\lambda\,\theta_1 g_\phi^0 - (aV+\kappa)\partial_\eta \phi_0. \tag{45}$$

Differentiating Eq. (41) with respect to η, one finds that $\partial_\eta \phi_0$ is a solution of the homogeneous part of Eq. (45). The solvability condition (Fredholm alternative) thus leads to a fifth relation:

$$\int d\eta\, \partial_\eta \phi_0 [\lambda\,\theta_1 g_\phi^0 + (aV+\kappa)\partial_\eta \phi_0] = 0. \tag{46}$$

With these five equations, we eliminate the two constants A_1 and B_1 and obtain three relations between the quantities $\theta_{1\pm}^{out}$ and $\partial_r \theta_{0\pm}^{out}$. One of them accounts for global mass conservation:

$$V = \frac{-1}{[h^0]_-^+}(D\,\partial_r \theta_{0+}^{out} - D\,\partial_r \theta_{0-}^{out}). \tag{47}$$

Choosing $[h^0]_-^+ = h_+^0 - h_-^0 = -1$, Eq. (7) of the discontinuous model is retrieved. Since it corresponds to a higher order contribution in W, the term $V(\theta_+ - \theta_-)$ is absent here.

Two other equations account for the kinetic boundary conditions. Since $\theta_{0\pm}^{out} = \theta_{eq}$, one has $W\theta_{1\pm}^{out} = \theta_\pm^{out} - \theta_{eq}$, to leading order. We then find on the $+$ side

$$\begin{aligned}(\theta_+^{out} - \theta_{eq}) - \xi\,\partial_r \theta_+^{out} = W\kappa \frac{-1}{\lambda [g^0]_-^+}\int d\eta (\partial_\eta \phi_0)^2 \\ + WV\left[\frac{-a}{\lambda[g^0]_-^+}\int d\eta (\partial_\eta\phi_0)^2 \right. \\ \left. - \frac{1}{[g^0]_-^+}\int d\eta \frac{(g^0 - g_-^0)(h^0 - h_+^0)}{M^0}\right] \\ + D\,\partial_r \theta_+^{out}\left[\int_0^{+\infty} d\eta \left(\frac{1}{M^0} - \frac{1}{D}\right)\right. \\ \left. + \frac{1}{[g_0]_-^+}\int d\eta \frac{g^0 - G^0}{M_0}\right],\end{aligned} \tag{48}$$

where $G^0 = g_+^0$ when $\eta > 0$ and $G^0 = g_-^0$ when $\eta < 0$. We have also defined $\xi = W\overline{\eta}$. On the $-$ side to first order

$$\begin{aligned}(\theta_-^{out} - \theta_{eq}) - \xi\,\partial_r \theta_-^{out} = W\kappa \frac{-1}{\lambda [g^0]_-^+}\int d\eta (\partial_\eta \phi_0)^2 \\ + WV\left[\frac{-a}{\lambda[g^0]_-^+}\int d\eta (\partial_\eta\phi_0)^2 \right. \\ \left. - \frac{1}{[g^0]_-^+}\int d\eta \frac{(g^0 - g_+^0)(h^0 - h_-^0)}{M^0}\right] \\ + D\,\partial_r \theta_-^{out}\left[-\int_{-\infty}^0 d\eta \left(\frac{1}{M^0} - \frac{1}{D}\right)\right. \\ \left. + \frac{1}{[g^0]_-^+}\int d\eta \frac{g^0 - G^0}{M^0}\right].\end{aligned} \tag{49}$$

These equations are identical to the kinetic boundary conditions, Eqs. (12), to leading order in $(\theta - \theta_{eq})$. We then obtain a set of equations that relates the parameters of the discontinuous model $(\tilde{\nu}_\pm, \tilde{\beta}, \theta_{eq}\Gamma)$ to the functions (f,g,h,M) of the phase field model. These relations impose that

$$h^0 = (1-\chi)\,\theta_{eq}\frac{M^0}{D} - \frac{g^0}{[g^0]_-^+} + h_*^0, \tag{50}$$

where h_*^0 is a function of ϕ, which must satisfy

$$\int_{-\infty}^{+\infty} d\eta \frac{h_*^0}{M^0} = 0. \tag{51}$$

Following the same arguments as in Ref. [14], we show in Appendix B that Eq. (50) corresponds to a variational phase field model at thermodynamic equilibrium only if $\chi = 1$ and $h_*^0 = 0$. The model with $\chi = 0$ does not correspond, in general, to a variational phase field model at equilibrium.

Let us now define the surface excess of a quantity Q as

$$(Q)_\xi = \int_{-\infty}^{\xi} dr (Q - Q_-) + \int_\xi^{+\infty} dr (Q - Q_+), \tag{52}$$

where $Q_\pm = \lim_{\eta \to \pm\infty} Q$. The general solution then reads

$$\frac{1}{\tilde{\nu}_+} = \frac{-1}{[g^0]_-^+}\left[-\frac{1}{D}(g^0)_\xi + W\int d\eta \left(\frac{1}{M^0} - \frac{1}{D}\right)(g_-^0 - g^0)\right], \tag{53}$$

$$\frac{1}{\tilde{\nu}_-} = \frac{-1}{[g^0]_-^+}\left[\frac{1}{D}(g^0)_\xi + W\int d\eta \left(\frac{1}{M^0} - \frac{1}{D}\right)(g^0 - g_+^0)\right], \tag{54}$$

$$\tilde{\beta} = \frac{-1}{[g^0]_-^+}\left[(1-\chi)\frac{\theta_{eq}}{D}(g^0)_\xi + (a - a^*)\frac{W}{\lambda}\int d\eta (\partial_\eta \phi_0)^2\right], \tag{55}$$

$$\theta_{eq}\Gamma = \frac{-W}{\lambda [g^0]_-^+}\int d\eta (\partial_\eta \phi_0)^2, \tag{56}$$

where

$$a^*=\frac{-\lambda[g^0]^+_-}{\int d\eta(\partial_\eta\phi_0)^2}\left[\frac{1}{([g^0]^+_-)^2}\int d\eta\frac{(g^0_+-g^0)(g^0-g^0_-)}{M^0}\right.$$
$$\left.+\frac{1}{[g^0]^+_-}\int d\eta\left(g^0-\frac{g^0_++g^0_-}{2}\right)\frac{h^0_*}{M^0}\right]. \quad (57)$$

We have obtained fast attachment-detachment kinetics: $\nu_\pm \sim 1/W$. Since $\tilde{\beta}\sim W$, we also find $\nu_0\sim 1/W$. Note that $\tilde{\beta}$ vanishes for an appropriate choice of a. The terms proportional to a and a^* in Eq. (55) come from, respectively, the finite relaxation time of the phase field and the finite diffusion constant in the step region. Note that the kinetic coefficients can be positive or negative.

4. Invariance of the kinetic boundary conditions when changing the interface reference point

Physical observations do not depend on the definition of the interface position ξ. Nevertheless, kinetic coefficients in Eqs. (53)–(55) explicitly depend on ξ via surface excess quantities $(g)_\xi$. This apparent paradox may be solved when looking carefully at the boundary conditions.

Let us first perform a change of the reference point in the boundary conditions of the discontinuous model. We want the concentration profile on the terraces to be invariant within this change of reference. Therefore, the concentration at the boundaries must transform as follows:

$$\theta^{(1)}_\pm=\theta^{(2)}_\pm-\Delta\xi\,\partial_r\theta^{(2)}_\pm+o((\Delta\xi)^2), \quad (58)$$

where indices (1) and (2) correspond to two different choices of interface at ξ_1 or ξ_2 with $\xi_2-\xi_1=\Delta\xi$. The first-order expansion in Eq. (58) is valid if $\Delta\xi\ll\ell_c$, where ℓ_c is a cutoff related to the diffusion of atom on terraces [e.g., the distance between steps or the desorption length $x_s=(D\tau)^{1/2}$]. In the kinetic boundary conditions of the discontinuous models Eq. (12), with reference ξ_1, we perform the substitution, Eq. (58). The obtained relations can be rewritten in the form of the usual boundary conditions, Eqs. (12), with reference ξ_2, and with new kinetic coefficients:

$$\frac{1}{\tilde{\nu}^{(2)}_+}=\frac{1}{\tilde{\nu}^{(1)}_+}+\frac{\Delta\xi}{D}, \quad (59)$$

$$\frac{1}{\tilde{\nu}^{(2)}_-}=\frac{1}{\tilde{\nu}^{(1)}_-}-\frac{\Delta\xi}{D}, \quad (60)$$

$$\tilde{\beta}^{(2)}=\tilde{\beta}^{(1)}+\frac{\Delta\xi}{D}\theta_{eq}(1-\chi). \quad (61)$$

Since it is not a kinetic quantity, $\theta_{eq}\Gamma$ is invariant under interface redefinition. The conditions under which such a rewriting is possible are

$$\tilde{\nu}_\pm\gg V,$$
$$\Delta\xi\ll\frac{1}{\kappa},$$
$$\frac{D}{\tilde{\nu}_\pm}\ll\ell_c. \quad (62)$$

One may then easily check that the kinetic coefficients of the thin interface limits Eqs. (53)–(55), obey the transformation rules, Eqs. (59)–(61). Indeed, in the frame of the thin interface asymptotics, conditions (62) are fulfilled: one has $\tilde{\nu}_\pm\sim D/W\gg V$, $\Delta\xi\sim W\ll 1/|\kappa|$, and $D/\tilde{\nu}_\pm\sim W\ll\ell_c$. Hence, we have shown that the transformation rules obeyed by the kinetic coefficients obtained from the thin interface limit leaves the physical behavior of the steps invariant when changing the step reference point ξ.

C. Sharp interface asymptotics

In the sharp interface asymptotics [13,7], the coupling constant is small $\lambda\sim W$. This leads to the same result as the thin interface asymptotics to zeroth order. To first order, θ_1 has to be replaced by $\overline{\theta_0}-\theta_{eq}$ in the solvability condition, Eq. (46). The resulting boundary condition,

$$\lambda[g_0]^+_-(\overline{\theta_0}-\theta_{eq})+W(av+\kappa)\int d\eta(\partial_\eta\phi_0)^2=0, \quad (63)$$

corresponds to the case of perfect transparency, Eq. (17) [an additional equation for mass conservation can be retrieved by integrating Eq. (43) only once with respect to η]. It is important to note that a variable mobility does not affect the final result. Comparing Eqs. (17) and (63), one obtains the following relations:

$$\beta=-a\frac{W}{\lambda[g^0]^+_-}\int d\eta(\partial_\eta\phi_0)^2, \quad (64)$$

$$\Gamma\theta_{eq}=\frac{-W}{\lambda[g_0]^+_-}\int d\eta(\partial_\eta\phi_0)^2. \quad (65)$$

The attachment kinetic coefficients are not large anymore. Within the sharp interface asymptotics, attachment kinetics is finite [i.e., $\beta\sim O(1)$], and steps are perfectly transparent $\nu_0\gg\nu_+,\nu_-$. As mentioned in Sec. II B, the kinetic asymmetry at steps (Ehrlich-Schwoebel effect) is irrelevant in this limit.

We also notice the absence of surface definition dependent terms [containing $(g)_\xi$] in the sharp interface asymptotics. These terms now lead to higher order contributions.

D. Domain of validity of the expansions

For the thin interface asymptotics to be valid, four conditions should to be fulfilled [14]:

$$|\kappa|W\ll 1, \quad (66)$$

$$\frac{WV}{D} \ll 1, \tag{67}$$

$$\lambda(\theta - \theta_{eq}) \ll 1, \tag{68}$$

$$\frac{\tau_p V}{W} \ll 1. \tag{69}$$

Furthermore, one has

$$\tilde{\nu}_{\pm} \sim \frac{D}{W}, \tag{70}$$

i.e., attachment kinetics is fast. This is, nevertheless, not the case in many situations of physical interest [15]. In Sec. IV, we will present a simple way to avoid this limitation.

The results of the sharp interface asymptotics can be retrieved by taking the limit $\lambda \sim W$ in the results of the thin interface asymptotics. One indeed retrieves Eq. (64) from Eq. (55) in the limit $a^* \sim \lambda \sim W \ll a$. This condition may be rewritten as $\lambda \ll D\tau_p / W^2$, and together with Eq. (65), implies that $\theta_{eq}\Gamma \gg W^3/(D\tau_p)$ in the sharp interface asymptotics, which is the condition obtained in Ref. [14].

E. Numerical simulations

In this section, the full numerical solution of the 2D phase field model (23) and (24) is presented. Since it has richer dynamics, we here focus on the thin interface asymptotics only. The reader interested in a comparison of the sharp interface asymptotics with a numerical solution of the phase field equations may refer to Ref. [20].

1. Step velocity

The velocity of a step in a periodic vicinal train was used as a first quantitative check of step kinetics. In order to force periodicity, one step only is used in a box which is periodic along the step and screw periodic in the direction perpendicular to steps. We have used the nonperiodic two-wells phase field model explicitly defined in Appendix C. (We have made some checks, with a periodic model, with several steps. We have also varied the lateral extent of the steps. This does not change the results.) We use the following parameters of the step model: $\Omega F = 10^{-2}$, $\tau^{-1} = 10^{-1}$, $D = 1$, $\theta_{eq} = 10^{-2}$, $\Gamma = 1$, and the distance between steps is $\ell = 5$. All results are in dimensionless units, which must be rescaled in order to retrieve the physical units. Using 10^2 Å and 10^4 s as spatial and temporal units, this simulation corresponds typically to growth of Si(111) at high temperature [21], where significant desorption is present.

We first used $\nu_0 = 0$ and vary the value of $d_+ = d_-$. For $W = 0.2$, the numerical integration with a simple Euler scheme was seen to converge for $W/dx = 4$ and $dt = 5 \times 10^{-2}$. The variation of the relative error on the step velocity, given the step model, is plotted as a function of $d_+ = d_-$ in Fig. 3. The results confirm condition (70), and show that the error is less than 1% when $d_+ / W \approx 1$ and less than 15% when $d_+ / W \approx 50$.

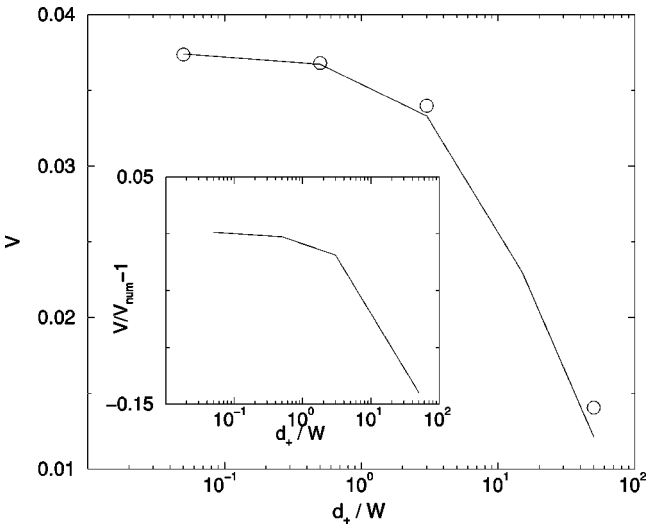

FIG. 3. Step velocity in the absence of Ehrlich-Schwoebel effect: $d_- = d_+$, and without transparency $\nu_0 = 0$, as a function of the attachment length d_+ / W. Relative error on the step velocity as a function of value of the attachment length d_+ / W.

Since $\lambda \sim W/(\Gamma \theta_{eq})$ and $\theta - \theta_{eq} \sim \beta v$ during growth, conditions (68) and (69) may be combined and read

$$\left(\frac{W}{D} + \beta\right)\frac{Wv}{\Gamma \theta_{eq}} \ll 1, \tag{71}$$

where we have used that $\tau_p \sim W^2 a^*/D \sim W^2\lambda/D \sim W^3/(D\Gamma\theta_{eq})$. The behavior of the velocity when varying Γ is plotted in Fig. 4. As predicted by Eq. (71), the convergence to the thin interface asymptotics breaks down when condition (71) is not fulfilled anymore.

The velocity of steps on a vicinal surface as a function of the distance between steps is plotted in Fig. 5. Good agreement with the prediction of the sharp interface model is observed.

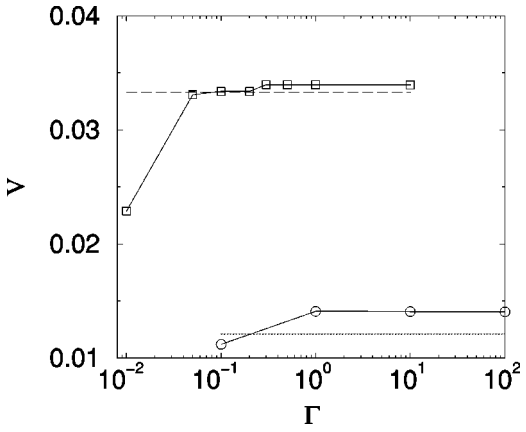

FIG. 4. Convergence of the velocity when varying Γ. Two cases are considered: $d = 0.1$ (squares) and $d = 10$ (circles). The value predicted by the thin interface asymptotics is shown in both cases. The convergence criterion of Eq. (71) reads $\Gamma \gg 0.15$ and $\Gamma \gg 1.0$ when $d = 0.1$ and $d = 10$, respectively.

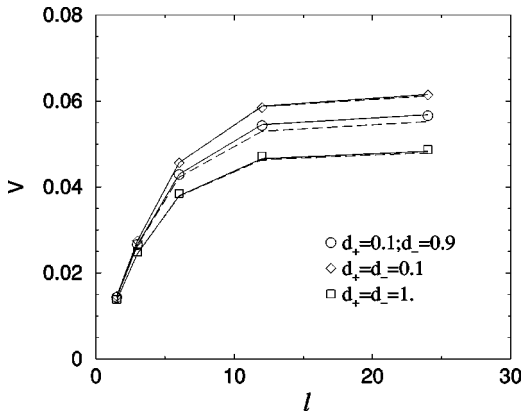

FIG. 5. Step velocity in a train of steps with one concentration field. The symbols are results of the numerical solution of the phase field. The solid lines correspond to the nonquasistatic prediction of the discontinuous model and the dashed lines to the quasistatic solution.

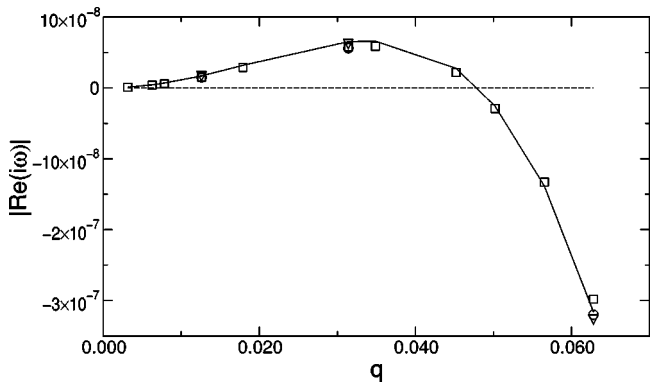

FIG. 6. Dispersion relation: growth rate of the meander $|\mathrm{Re}[i\omega]|$ as a function of the wave vector. The solid line is the quasistatic prediction from the discontinuous model. The squares indicate the result from the numerical solution of the phase field model with one concentration field when $\chi=1$. The circles and triangles indicate the numerical solution of the phase field model and the nonquasistatic prediction of the sharp interface model when $\chi=0$.

2. Linear stability analysis

The consequences of the Ehrlich-Schwoebel effect on surface dynamics vanish when $\nu_{\pm}$ are large. Since this is in fact the domain of validity of the thin interface asymptotics, the accuracy of the Ehrlich-Schwoebel effect at the steps is not easy to probe. Nevertheless, due to the advances in visualization techniques and in the atomic control of the surface, it is nowadays possible to measure consequences of small Schwoebel effects. A recent example is the experimental discovery of a tiny Schwoebel effect on the Si(111) surface using island electromigration [5,22].

Here, we focus on the meandering instability at steps, which is directly proportional to the Ehrlich-Schwoebel effect [19]. The amplification rate is measured via the increase of the amplitude of a sinusoidal meander of fixed wavelength λ_m. We consider the in-phase mode, which is the most unstable mode, where all steps have the same meander. Thus, only one step, with periodic boundary conditions in the direction perpendicular to the step, is needed. A rectangular grid is used, which is useful in the long wavelength limit to account for three separate length scales: $W \ll \ell \ll \lambda_m$. We have used the parameters $W=0.1$, $\Omega F=10^{-4}$, $\tau^{-1}=10^{-4}$, $\theta_{eq}=10^{-2}$, $\Gamma=1$, $D=1$, $d_+=0.05$, $d_-=0.6$, $\nu_0=0$, $\ell=5$. The step velocity expected from the step model is then $V=4.94\times10^{-4}$, and the velocity of steps found from the numerical solution of the phase field model is $V=4.934\times10^{-4}$ when $dx=5\times10^{-2}$ and $dt=2\times10^{-4}$.

The amplification rate is plotted in Fig. 6 as a function of $q=2\pi/\lambda_m$. The accuracy is better than 10%. Note that we have chosen parameters that obey constraint (70).

A periodic model defined in Appendix C 2 was tested and leads to qualitatively similar results.

IV. PHASE FIELD MODEL WITH ONE CONCENTRATION FIELD PER TERRACE

A. Model equations for one step

In the presence of strong Ehrlich-Schwoebel [15] effect during growth or, in general, when kinetics is slow, a finite concentration jump may appear at the step. This situation cannot be tackled by a phase field model with one global concentration field. Indeed, in the sharp and thin interface limits of this model, the concentration jump at the step must be small. In this section, a phase field model whose sharp interface asymptotics is consistent with a finite concentration jump at the step is presented.

Going back to some more microscopic considerations, an extreme Ehrlich-Schwoebel effect corresponds to the case where the adatoms on the upper terrace in the vicinity of a step cannot attach to the step or go to the lower terrace, these adatoms behave as a phase which is disconnected from the lower terrace. To deal with such an extreme case, it is natural to consider that the concentration on both sides of the step correspond to two different fields. A phase field model with one concentration field on each terrace is therefore presented in this section. We will first focus on an isolated step. The case of a vicinal surface will be analyzed later.

We now want a continuum concentration that sits on one side of the step and which is zero on the other side. Therefore, the concentration has to relax to the form $\theta=\theta_0\psi$, where ψ is a smooth function of the phase field ϕ, with $\psi=0$ on one side of the step and $\psi=1$ on the other side. Instead of being proportional to the concentration gradient $\boldsymbol{\nabla}\theta$, the diffusion flux is now proportional to the Wronskian of θ and ψ:

$$J_d \sim \boldsymbol{\nabla}\frac{\theta}{\psi} \sim [\psi\boldsymbol{\nabla}\theta - \theta\boldsymbol{\nabla}\psi]. \tag{72}$$

In the step region, the concentrations on the upper and lower terraces are coupled by mass exchange with kinetic coefficients $\mathcal{B}_{\pm\pm}$. We have chosen the index $+$ for lower side of the step, and ψ is denoted by ϕ_+ on this side. The index

$-$ designates the upper side of the step. Mass conservation now reads for both terraces:[2]

$$\partial_t\theta_+ + \partial_t h_+ = D[\phi_+\nabla^2\theta_+ - \theta_+\nabla^2\phi_+] - \frac{1}{\tau}(\theta_+ - \theta_+^\infty) - (\mathcal{B}_{++}\theta_+ - \mathcal{B}_{+-}\theta_-), \tag{73}$$

$$\partial_t\theta_- + \partial_t h_- = D[\phi_-\nabla^2\theta_- - \theta_-\nabla^2\phi_-] - \frac{1}{\tau}(\theta_- - \theta_-^\infty) - (\mathcal{B}_{--}\theta_- - \mathcal{B}_{-+}\theta_+), \tag{74}$$

where τ, $\theta_\pm^\infty$, and $B_{\pm\pm}$ are functions of ϕ. Another equation is needed to determine the dynamics of the phase field itself:

$$\tau_\phi\,\partial_t\phi = W^2\nabla^2\phi - f_\phi + \lambda[g_{+\phi}(\theta_+ - \theta_{eq}\phi_+) + g_{-\phi}(\theta_- - \theta_{eq}\phi_-)], \tag{75}$$

where the coupling term (in brackets) comes from a direct analogy to Eq. (19). $g_\pm$ are to be chosen to ensure that neither the position nor the sharpness (curvature) of the minima of f are changed by the coupling term.

B. Sharp interface asymptotics

1. Expansion of the model equations

Following the same trend as in Sec. III, let us define the inner region as the location of rapid variations of ϕ and θ. In this region, Eqs. (73)–(75) are expanded for small W. In order to obtain the correct far-field limit, one needs

$$\lim_{\eta\to-\infty}\mathcal{B}_{\pm-} = 0, \tag{76}$$

$$\lim_{\eta\to+\infty}\mathcal{B}_{\pm+} = 0, \tag{77}$$

$$\lim_{\eta\to\pm\infty}\theta_\pm^\infty = \Omega\tau F \equiv \theta^\infty. \tag{78}$$

Moreover, we choose $\mathcal{B}\sim|\nabla\phi|$. This leads to $\mathcal{B}=DN/W$, where N is of the order of 1. Let us call ℓ_c the smallest macroscopic cutoff length associated with the diffusion field. Our small parameter is once again $\epsilon = W/\ell_c$, and we define the inner variable η as previously. We now rescale all lengths by ℓ_c (which amounts to take $\ell_c = 1$ in all equations and $\epsilon = W$). Expanded up to first order, the phase field equations, Eqs. (73)–(75), read

$$(\partial_\eta + W\kappa)[\phi_+\,\partial_\eta\theta_+ - \theta_+\,\partial_\eta\phi_+] - W(N_{++}\theta_+ - N_{+-}\theta_-) + \frac{WV}{D}\partial_\eta(\theta_+ + h_+) = o(W^2), \tag{79}$$

$$(\partial_\eta + W\kappa)[\phi_-\,\partial_\eta\theta_- - \theta_-\,\partial_\eta\phi_-] - W(N_{--}\theta_- - N_{-+}\theta_+) + \frac{WV}{D}\partial_\eta(\theta_- + h_-) = o(W^2), \tag{80}$$

$$\partial_{\eta\eta}\phi - f_\phi + \lambda[g_{+\phi}(\theta_+ - \theta_{eq}\phi_+) + g_{-\phi}(\theta_- - \theta_{eq}\phi_-)] + W(aV+\kappa)\partial_\eta\phi = o(W^2). \tag{81}$$

2. Zeroth order

To zeroth order, Eqs. (80) and (79) provide

$$\phi_-^0\,\partial_\eta\theta_{-0} - \theta_{-0}\,\partial_\eta\phi_-^0 = B_{0-},$$

$$\phi_+^0\,\partial_\eta\theta_{+0} - \theta_{+0}\,\partial_\eta\phi_+^0 = B_{0+}, \tag{82}$$

where $B_{0\pm}$ are constants. From matching conditions, $\partial_\eta\theta_0, \partial_\eta\phi_0 \to 0$ when $\eta\to\pm\infty$. Thus, $B_{0\pm}=0$, and

$$\theta_{-0} = \tilde{\theta}_{-0}\phi_-^0,$$

$$\theta_{+0} = \tilde{\theta}_{+0}\phi_+^0, \tag{83}$$

where $\tilde{\theta}_{\pm0}$ are arbitrary constants. From the matching conditions (33), $\tilde{\theta}_{0\pm} = \theta_{0\pm}^{out}$.

To leading order, Eq. (81) reads

$$\partial_{\eta\eta}\phi_0 - f_\phi^0 = 0. \tag{84}$$

This equation is once again analogous to the sine-Gordon equation. It has solitonlike kink solutions (the steps) going from one minima of f to the next one. Note that using the thin interface asymptotics here is not appropriate. Indeed, this would require $\theta_{0\pm} = \theta_{eq}\phi_\pm$, which is just what we want to avoid. The sharp interface asymptotics is the adapted choice because it leaves $\theta_{0\pm}^{out}$ undetermined.

3. First order

The relevant information for dynamics appears to first order. Equation (80) now reads

$$\partial_\eta[\phi_-^0\,\partial_\eta\theta_{1-} - \theta_{1-}\,\partial_\eta\phi_-^0 + \phi_1\phi_{-\phi}^0\,\partial_\eta\theta_{0-} - \theta_{0-}\,\partial_\eta(\phi_1\phi_{-\phi}^0)] - (N_{--}^0\theta_{0-} - N_{-+}^0\theta_{0+}) + \frac{V}{D}\partial_\eta(\theta_{0-} + h_-^0) = 0. \tag{85}$$

From Eqs. (76) and (77), one has $\lim_{\eta\to\pm\infty}N_{-\pm} = 0$. Thus, taking the limit $\eta\to\pm\infty$ in Eq (85) leaves $\tilde{\theta}_{0\pm}$ undetermined. Equation (85) is integrated with respect to η. One finds

[2]The diffusion terms in brackets are easily generalized to the case of a nonconstant mobility. This leads to a term of the form $\nabla[\mathcal{M}_+(\phi_+\nabla\theta_+ - \theta_+\nabla\phi_+)]$. Since the variations of the mobilities $\mathcal{M}_\pm$ do not affect the sharp interface asymptotics presented in the following, we do not consider this generalization.

$$\phi^0_- \partial_\eta \theta_{1-} - \theta_{1-} \partial_\eta \phi^0_- + \phi_1 \phi^0_{-\phi} \partial_\eta \theta_{0-} - \theta_{0-} \partial_\eta (\phi_1 \phi^0_{-\phi}) - \left[\tilde{\theta}_{0-} \left(\int_{+\infty}^{\eta} d\eta N^0_{--} \phi^0_- \right) - \tilde{\theta}_{0+} \left(\int_{+\infty}^{\eta} d\eta N^0_{-+} \phi^0_+ \right) \right] + \frac{V}{D} (\theta_{0-} + h^0_- - h^0_{-+}) = B_1 . \quad (86)$$

Here, $h_{-+} = \lim_{\eta \to +\infty} h_-$. In the limit where $\eta \to +\infty$, one has $\partial_\eta \phi_0 \to 0$ from matching conditions. Hence, the left-hand side of Eq. (86) is zero. Therefore, $B_1 = 0$. Since ϕ^{out} is constant in the outer space, one has $\partial_\eta \phi_1 \to 0$ as $\eta \to -\infty$. Thus, one finds the kinetic boundary condition

$$D \partial_\eta \theta_{1-} + v \tilde{\theta}_{0-} = V[h^0_-]^+_- + \left[\tilde{\theta}_{0-} \left(D \int_{+\infty}^{-\infty} d\eta N^0_{--} \phi^0_- \right) - \tilde{\theta}_{0+} \left(D \int_{+\infty}^{-\infty} d\eta N^0_{-+} \phi^0_+ \right) \right], \quad (87)$$

which may be written as a condition equivalent to Eq. (18)

$$D \partial_r \theta^{out}_{0-} + V \theta^{out}_{0-} = (\alpha - 1 + \theta_{eq} \chi) V + \nu (\theta^{out}_{0+} - \theta^{out}_{0-}), \quad (88)$$

provided that

$$\nu = D \int_{-\infty}^{+\infty} d\eta N^0_{--} \phi^0_- = D \int_{-\infty}^{+\infty} d\eta N^0_{-+} \phi^0_+ , \quad (89)$$

$$1 - \alpha = -[h^0_-]^+_- + \chi \theta_{eq} . \quad (90)$$

Using the same method for the other side of the step leads to

$$D \partial_r \theta^{out}_{0+} + V \theta^{out}_{0+} = (\alpha + \chi \theta_{eq}) V + \nu (\theta^{out}_{0+} - \theta^{out}_{0-}), \quad (91)$$

where we have used

$$\nu = D \int_{-\infty}^{+\infty} d\eta N^0_{+-} \phi^0_- = D \int_{-\infty}^{+\infty} d\eta N^0_{++} \phi^0_+ , \quad (92)$$

$$\alpha = -[h^0_+]^+_- - \chi \theta_{eq} . \quad (93)$$

Combining Eqs. (90) and (93), we find

$$[h_+ + h_-]^+_- = -1, \quad (94)$$

which is expected since $h_+ + h_-$ is interpreted as the concentration of solid in the layer bounded by the step. Following the same line as for the phase field model, with one concentration field, Eqs. (90) and (93) show that the phase field model Eqs. (73) and (75), is variational at equilibrium only if $\chi = 1$. This analysis is performed in detail in Appendix B.

In order to recover the third boundary condition of the discontinuous model, let us first note the formal similarity between the first order contributions in Eqs. (81) and (84) differentiated with respect to η

$$\partial_{\eta\eta} (\partial_\eta \phi_0) - f^0_{\phi\phi} \partial_\eta \phi_0 = 0, \quad (95)$$

$$\partial_{\eta\eta} \phi_1 - f^0_{\phi\phi} \phi_1 = \frac{\lambda}{W} [g^0_{+\phi} (\theta_{0+} - \theta_{eq} \phi_+) + g^0_{-\phi} (\theta_{0-} - \theta_{eq} \phi_-)] - (av + \kappa) \partial_\eta \phi_0 . \quad (96)$$

The solvability condition (or Fredholm alternative) then indicates that the right-hand side of the second equation should be orthogonal to the the solution of the homogeneous equation:

$$\int d\eta \, \partial_\eta \phi_0 \left[\frac{\lambda}{W} [g^0_{+\phi} (\theta_{0+} - \theta_{eq} \phi_+) + g^0_{-\phi} (\theta_{0-} - \theta_{eq} \phi_-)] - (aV + \kappa) \partial_\eta \phi_0 \right] = 0. \quad (97)$$

The integration provides

$$\left(\int d\phi \, g^0_{+\phi} \phi^0_+ \right) (\tilde{\theta}_{0+} - \theta_{eq}) + \left(\int d\phi \, g^0_{-\phi} \phi^0_- \right) (\tilde{\theta}_{0-} - \theta_{eq}) - \frac{W}{\lambda} (aV + \kappa) \int d\eta (\partial_\eta \phi_0)^2 = 0. \quad (98)$$

Comparing this equation to the boundary condition, Eq. (19), three relations are obtained:

$$\alpha = \frac{1}{\mathcal{G}} \int d\phi \, g^0_{+\phi} \phi^0_+ = 1 - \frac{1}{\mathcal{G}} \int d\phi \, g^0_{-\phi} \phi^0_- , \quad (99)$$

$$\beta = \frac{aW}{\lambda \mathcal{G}} \int d\eta (\partial_\eta \phi_0)^2, \quad (100)$$

$$\Gamma \theta_{eq} = \frac{W}{\lambda \mathcal{G}} \int d\eta (\partial_\eta \phi_0)^2, \quad (101)$$

where

$$\mathcal{G} = \int d\phi (g^0_{+\phi} \phi^0_+ + g^0_{-\phi} \phi^0_-). \quad (102)$$

In summary, the sharp interface asymptotics provides a link between the phase field model and the discontinuous model. The coefficients of the boundary conditions are given by Eqs. (89), (90), (92), (93), (99), (100), and (101). Since none of these parameters scale with W, the sharp interface limit of the phase field model with one concentration field per terrace leads to a discontinuous step model with arbitrary kinetics. Note that combining Eqs. (100) and (101), the step diffusion constant is found to be equal to [5]

$$\frac{1}{a} = \frac{W^2}{\tau_\phi} = (\nu_+ + \nu_-) \Gamma \theta_{eq} = \frac{\Gamma \theta_{eq}}{\beta} . \quad (103)$$

C. More than one step

A direct extension of the previous model to the case of a surface with an arbitrary number of steps is to use one concentration field per layer. The set of model equations would then be written as

$$\partial_t \theta_n + \partial_t h_n = D[\psi_n \nabla^2 \theta_n - \theta_n \nabla^2 \psi_n] + \frac{1}{\tau}(\theta_n^\infty - \theta_n) - [\theta_n(\mathcal{B}^n_{++} + \mathcal{B}^n_{--}) - \theta_{n-1}\mathcal{B}^n_{-+} - \theta_{n+1}\mathcal{B}^n_{+-}], \tag{104}$$

where h_n, ψ_n, and $\mathcal{B}^n_{\pm\pm}$ are smooth functions of ϕ. $h_n = h_+$ close to the upper step at the edge of the terrace of height n and $h_n = h_-$ in the vicinity of the lower step. ψ_n is equal to one on the nth terrace and zero elsewhere. An additional equation determines the dynamics of the phase field itself

$$\tau_\phi \partial_t \phi = W^2 \nabla^2 \phi - f_\phi + \lambda W \sum_n g_{n\phi}(\theta_n - \theta_{eq}\psi_n), \tag{105}$$

where $g_{n\phi}$ is a function of ϕ. The sharp interface asymptotics of this model around one step is the same as what was presented in the preceding section. Therefore, model equations (104) and (105) correspond to a stepped surface with an arbitrary number of steps.

D. Numerical simulations

1. Three fields model

On a stepped surface, a large number of concentration fields might be numerically difficult to handle. We present in this section a trick to avoid this unlimited number of concentration fields. The idea is simple. We only use two concentration fields, each one is used for every other terrace. The model equations now read

$$D[\phi_+^* \nabla^2 \theta_+ - \theta_+ \nabla^2 \phi_+^*] + (\mathcal{B}^*_{++}\theta_+ - \mathcal{B}^*_{+-}\theta_-) + \frac{1}{\tau}(\theta_+^{*\infty} - \theta_+) = \partial_t \theta_+ + \partial_t h_+^*, \tag{106}$$

$$D[\phi_-^* \nabla^2 \theta_- - \theta_- \nabla^2 \phi_-^*] + (\mathcal{B}^*_{--}\theta_- - \mathcal{B}^*_{-+}\theta_+) + \frac{1}{\tau}(\theta_-^{*\infty} - \theta_-) = \partial_t \theta_- + \partial_t h_-^*, \tag{107}$$

$$W^2 \nabla^2 \phi - f_\phi - \lambda W[g^*_{+\phi}(\theta_+ - \theta_{eq}\phi_+^*) + g^*_{-\phi}(\theta_- - \theta_{eq}\phi_-^*)] = \tau_\phi \partial_t \phi, \tag{108}$$

where quantities with "*" change value from one step to the other, e.g.,

$$\phi_\sigma^* = \frac{1+z}{2}\phi_\sigma + \frac{1-z}{2}\phi_{-\sigma}, \tag{109}$$

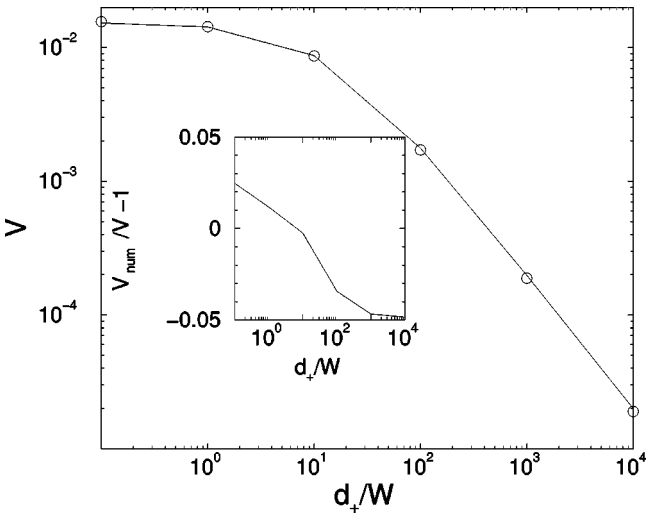

FIG. 7. Same as Fig. 3, but using the phase field model with one concentration field per terrace. Parameters: $W=1$, $\Omega F = 10^{-3}$, $D=1$, $\nu_0 = 0$, $\theta_{eq} = 10^{-5}$, $\Gamma = 10^4$, $\tau^{-1} = 10^{-3}$ (circles), and $\tau^{-1} = 10^{-2}$ (squares).

$$\mathcal{B}^*_{\sigma_1,\sigma_2} = \frac{1+z}{2}\mathcal{B}_{\sigma_1,\sigma_2} + \frac{1-z}{2}\mathcal{B}_{-\sigma_1,-\sigma_2}, \tag{110}$$

where $\sigma, \sigma_1, \sigma_2 = \pm 1$. $z = \pm 1$ is a periodic function of ϕ, whose period is two times that of the periodic potential f. z changes sign each time ϕ goes through a minimum of f (which corresponds to a terrace). $\theta_\pm^{*\infty}$ and $h_\pm^*$ also obey Eq. (109). Explicit examples are given in Appendix D. Once again, the sharp interface asymptotics of this model around one step is clearly the same as that presented in the case of an isolated step.

A numerical solution of the three fields model was performed using a simple Euler scheme in time and second-order finite differences in space, with time step dt and grid lattice unit dx. The model parameters are that calculated in Appendix D 1 b. The equations were solved on a rectangular lattice, where the lattice parameter along the average step direction is adjusted to the numerical needs.

2. Step velocity

We first check the velocity of straight steps on a grid having a few points in the direction x along the step and 101 points in the other direction. We have checked that changing the number of points in the lateral direction does not affect the result (when steps are stable with respect to meandering). We have also checked that the number of steps in a regular vicinal surface does not affect the velocity (when the surface is stable with respect to step bunching).

The first result that we have checked is the agreement of the step velocity with the prediction of the discontinuous model as a function of the kinetic coefficients. As shown in Fig. 7, quantitative agreement is found over five orders of magnitude. We have also checked the saturation of the step velocity when the interstep distance is larger than the desorption length $x_s = \sqrt{D\tau}$ (see Fig. 8). We find very good agreement with the nonquasistatic prediction of Appendix E. Mod-

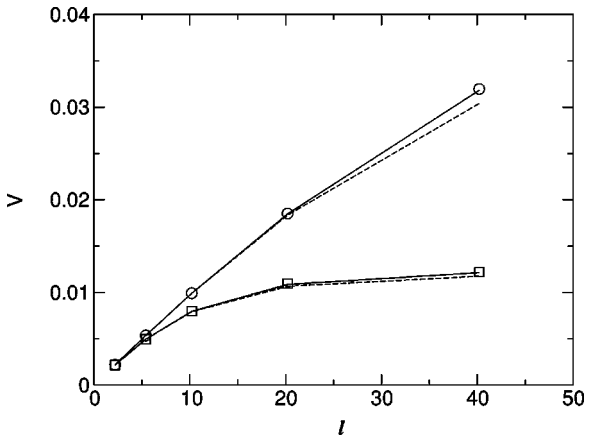

FIG. 8. Same as Fig. 5, but using the phase field model with one concentration field per terrace. Parameters: $W=1$, $\Omega F=10^{-3}$, $D=1$, $\nu_+^{-1}=0.1$, $\nu_-^{-1}=39.9$, $\nu_0=0$, $\theta_{eq}=10^{-5}$, $\Gamma=10^{-4}$, $\tau^{-1}=10^{-3}$ (circles), and $\tau^{-1}=10^{-2}$ (squares).

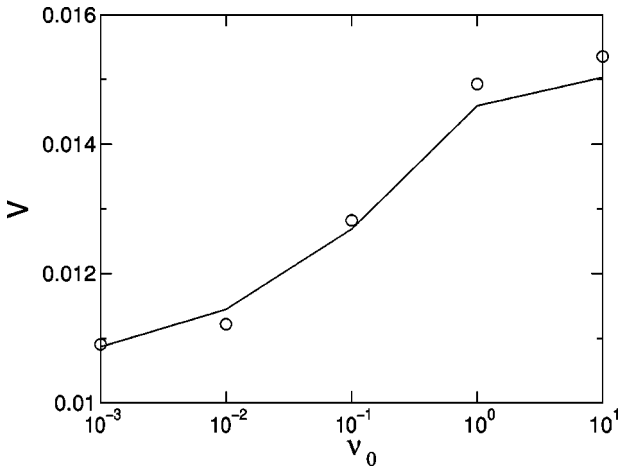

FIG. 10. Step velocity as a function of step transparency. Phase field model with two concentration fields. Same parameters as in Fig. 9, with ν_0 varying and $\alpha=0.995$.

els *A* and *B* lead to identical results.

The consequences of the Ehrlich-Schwoebel effect on step velocity were then checked. Once again, good agreement is found with the predictions of the discontinuous model (see Fig. 9).

Transparency also affects step velocity. As shown in Fig. 10, varying the kinetic coefficient ν_0 affects the velocity of a straight step, in agreement with discontinuous model predictions.

3. Linear stability analysis

The dispersion relation of the in-phase meander of a train of steps in the presence of Ehrlich-Schwoebel effect was also studied. The growth rate corresponding to a given wavelength is calculated by fitting the evolution of the amplitude of a small sinusoidal perturbation. The results are plotted in Fig. 11. Quantitative agreement is found at long wavelengths. A deviation at short length scales was seen. This deviation vanishes as *W* gets smaller. From this result, we conclude that kinetics is taken into account for relatively large values of *W*. Nevertheless, sharper interfaces are needed for an accurate description of line tension.

To check the bunching rate, we restricted the analysis to step pairing: the increase or decrease of a perturbation of the position of one step in a box with two initially equidistant steps was measured. This corresponds to the mode $\varphi=\pi$ in the dispersion relation (see Appendix E). The results of the phase field model during growth and sublimation are in quantitative agreement with the discontinuous model, as shown in Fig. 12.

4. Nonlinear dynamics

We now focus on the behavior of the step meander in the nonlinear regime. It was shown from multiscale analysis [3] that step meander should exhibit spatiotemporal chaos in the presence of significant desorption and close to the instability threshold. This result is confirmed by our simulations, as shown in Fig. 13.

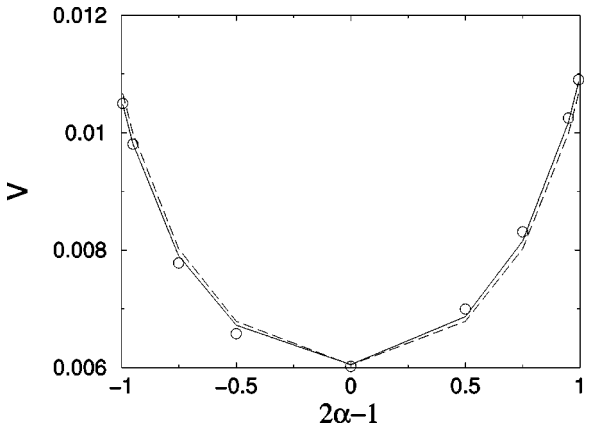

FIG. 9. Step velocity as a function of the asymmetry in attachment kinetics $2\alpha-1$, with $\nu_+^{-1}+\nu_-^{-1}=40$. Phase field model with one concentration field per terrace. Parameters: $W=1$, $\Omega F=10^{-3}$, $\tau^{-1}=10^{-2}$, $D=1$, $\nu_0=0$, $\theta_{eq}=10^{-5}$, $\Gamma=10^{4}$, $\ell=20.2$.

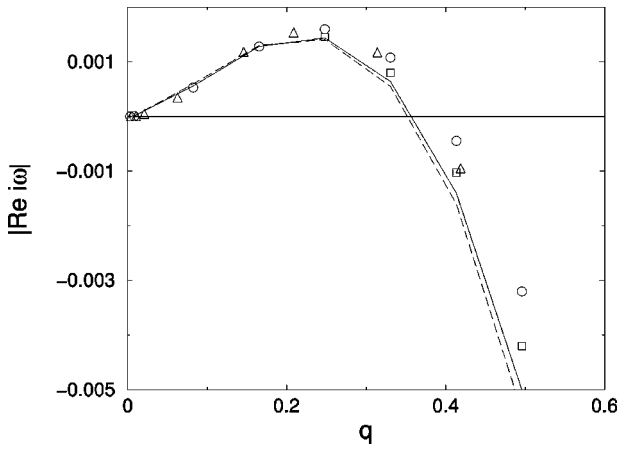

FIG. 11. Growth rate of in-phase step meander in the linear regime, as a function of the wave vector. Same parameters as in Fig. 7, but with $\tau^{-1}=10^{-6}$. Circles correspond to $W=1$ and $\chi=0$, squares to $W=0.5$ and $\chi=0$, and triangles to $W=0.5$ and $\chi=1$.

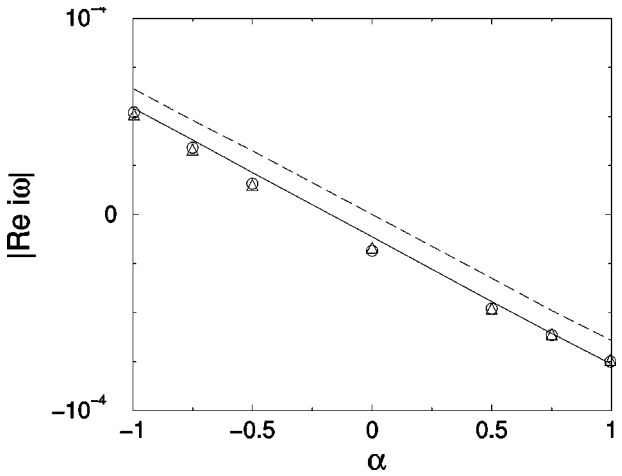

FIG. 12. Pairing rate as a function of α (i.e., the Ehrlich-Schwoebel effect), with $\nu_+^{-1}+\nu_-^{-1}=40$. Circles correspond to $\chi=0$ and triangles to $\chi=1$. Parameters: $W=1$, $\Omega F=10^{-4}$, $\tau^{-1}=10^{-6}$, $D=1$, $\nu_0=0$, $\theta_{eq}=10^{-5}$, $\Gamma=10^4$, $\ell=30.15$.

V. CONCLUSION

In this paper, we have first discussed the discontinuous step model. Several reformulations of the boundary conditions at the steps were presented. The limit of perfect step transparency $\nu_0\to\infty$ was shown to correspond to kinetic boundary conditions used in solidification. Moreover, step transparency may be incorporated in the step model as a correction to the equilibrium concentration due to step motion. The general stability analysis of a vicinal surface during growth was performed within the framework of the discontinuous model.

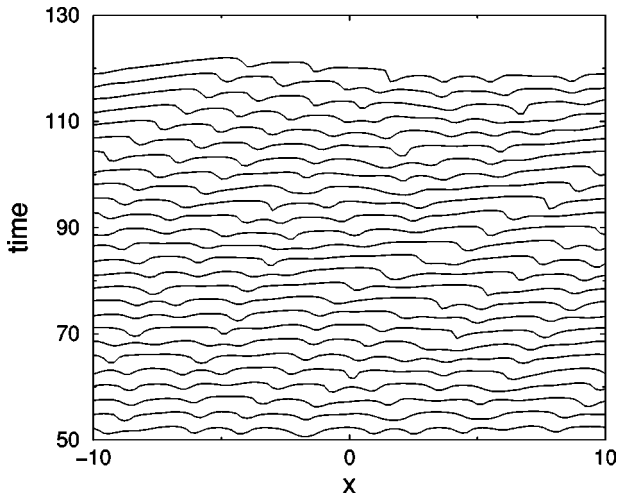

FIG. 13. Full numerical solution of the 2D phase field model with Ehrlich-Schwoebel effect and significant desorption. Kuramoto-Sivashinsky-like chaos of the meander of an isolated step. The front is presented at different times. Time units are arbitrary. Parameters are $W=0.3$, $\Gamma=10^3$, $\Omega F=2\times10^{-2}$, $\theta_{eq}=10^{-5}$, $\tau=1$, $D=1$ $\nu_+^{-1}=0.1$, $\nu_-^{-1}=20$, $dt=10^{-2}$, $dx=0.2$. The supersaturation is defined as $\sigma=F\tau/c_{eq}-1$. The critical super saturation for the morphological instability to appear is $\sigma_c=2.3\times10^3$, the simulation is performed with $\sigma=5\times10^3$.

A phase field model with one global concentration field was then studied. We have performed the *thin interface asymptotics*, where the departure from equilibrium at the interface is chosen to be small *a priori*. This leads to a discontinuous model with fast kinetics (Indeed, fast kinetics is needed in order to keep the smallness of the departure from equilibrium at the interface). Since kinetics is fast, the interface definition appears explicitly in the expression of the kinetic coefficients. This dependence is consistent with the independence of step dynamics with respect to a change in the interface reference point. Thus, as opposed to Ref. [12], we have well defined kinetic coefficients, even in the case of fast kinetics. The numerical simulation of the phase field model is in agreement with the predictions from the discontinuous model. But the Schwoebel effect is difficult to probe due to fast kinetics. The *sharp interface asymptotics* is an expansion in the weak coupling limit. It therefore leads to a discontinuous model with strong step transparency.

We have finally shown that a model with one concentration field per terrace allows one to recover arbitrary step kinetics, i.e., arbitrary strong Erhlich-Schwoebel effect and step transparency. The numerical simulation of this phase field model is in quantitative agreement with the predictions of the discontinuous model over at least five orders of magnitude of variation of the kinetic coefficients. The occurrence of chaos, predicted from a multiscale analysis of the discontinuous model for an isolated step during growth with significant desorption was checked.

The kinetic boundary condition with equilibrium reference state ($\chi=1$) was found to be the only one that corresponds to variational dynamics at equilibrium in both types of phase field models. Thus, the model with adatom vacuum reference state ($\chi=0$) does not seem to be thermodynamically consistent.

To the best of our knowledge, the phase field model with one concentration field per terrace is a new model. This model may be relevant for heteroepitaxy: a straightforward generalization is obtained by choosing a diffusion constant of the adatoms that depends on the layer where they are located. This may be relevant for solidification when diffusivities in the solid and liquid phases are different. Indeed, this would avoid incorporating nonvariational additional terms in the phase field model [23].

More generally, the phase field model with Wronskian diffusion flux, Eq. (72), is a powerful method to treat diffusion problems in a domain limited by moving boundaries or in problems of diffusive relaxation to a field which depends on space and time.

As natural perspective for this work, an analysis of step collision, annihilation, and nucleation dynamics would complete a full description of a growing crystal surface.

ACKNOWLEDGMENTS

The author wishes to thank C. Misbah, K. Kassner, P. Berger, and T. Biben for useful discussions.

APPENDIX A: VARIABLE EQUILIBRIUM CONCENTRATION

The equilibrium concentration θ_{eq} is, in general, not constant in the vicinity of the step region. Nevertheless, θ_{eq} has

to be constant far from the step (here, we neglect any long range interactions—such as the ones of elastic origin). The modified phase field model with a ϕ-dependent equilibrium concentration reads

$$\partial_t \theta = \nabla\left[M \nabla\left(\frac{\theta - \theta_{eq}}{\Psi} \right)\right] + \Omega F - \frac{\theta}{\tau} - \partial_t h, \tag{A1}$$

$$\tau_p\, \partial_t \phi = W^2 \nabla^2 \phi - f_\phi + \lambda \left(\frac{\theta - \theta_{eq}}{\Psi} \right) g_\phi, \tag{A2}$$

with $\Psi = \theta_{eq} / \overline{\theta}_{eq}$, where $\overline{\theta}_{eq}$ is the value of θ_{eq} far from the step. Using a similar expansion as for the model with constant equilibrium concentration, one finds a result similar to that of Sec. III. The main point is that the solid reference concentration must be replaced by a generalized reference concentration $h + \theta_{eq}$. Thus, the expression of the kinetic coefficients (53)–(57) is unchanged, except that we now have a new condition,

$$h^0 + \theta^0_{eq} = -\frac{g^0}{[g^0]^+_-} + (1-\chi)\overline{\theta}_{eq}\frac{M}{D} + h_*, \tag{A3}$$

which replaces Eq. (50), where h_* must satisfy relation (51).

APPENDIX B: VARIATIONAL CHARACTER OF THE PHASE FIELD MODELS AT THERMODYNAMIC EQUILIBRIUM

1. Model with one concentration field

Let us start with the energy functional

$$\mathcal{F} = \int d\mathbf{x} \left[\frac{W^2}{2} (\nabla \phi)^2 + f + \frac{\lambda \overline{\theta}_{eq}}{2\theta_{eq}} (\theta - \theta_{eq})^2 \right], \tag{B1}$$

where $d\mathbf{x}$ is the surface element, θ_{eq} is a function of ϕ, and $\overline{\theta}_{eq}$ is the constant value of θ_{eq} far from the steps. We now define the total concentration (i.e., adatom gas plus solid)

$$U = \theta + h. \tag{B2}$$

Suppose that

$$h = -\frac{g}{[g]^+_-}, \tag{B3}$$

up to an arbitrary additive constant. One can then easily check that, up to higher order terms $\sim(\theta - \theta_{eq})^2$, the phase field model with one concentration field, Eqs. (23) and (24), may be written at equilibrium, when $\theta^\infty = \theta_{eq}$:

$$\lambda\, \partial_t U = \nabla\left[M \nabla\left(\left.\frac{\delta \mathcal{F}}{\delta U}\right|_\phi \right)\right] - \frac{1}{\tau} \left.\frac{\delta \mathcal{F}}{\delta U}\right|_\phi, \tag{B4}$$

$$\partial_t \phi = -\frac{1}{\tau_p} \left.\frac{\delta \mathcal{F}}{\delta \phi}\right|_U. \tag{B5}$$

This set of equations then decrease the functional $\mathcal{F}$ over the course of time. Indeed, up to boundary terms at the frontier of the integration domain, one has

$$\begin{aligned} \frac{d\mathcal{F}}{dt} &= \int d\mathbf{x} \left[\partial_t \phi \left.\frac{\delta \mathcal{F}}{\delta \phi}\right|_U + \partial_t U \left.\frac{\delta \mathcal{F}}{\delta U}\right|_\phi \right] \\ &= \int d\mathbf{x} \left[-\frac{1}{\tau_p} \left(\left.\frac{\delta \mathcal{F}}{\delta \phi}\right|_U \right)^2 - \frac{M}{\lambda} \left(\nabla \left.\frac{\delta \mathcal{F}}{\delta U}\right|_\phi \right)^2 \right. \\ &\quad \left. - \frac{1}{\tau\lambda} \left(\left.\frac{\delta \mathcal{F}}{\delta U}\right|_\phi \right)^2 \right] \leqslant 0. \end{aligned} \tag{B6}$$

When $\chi = 1$, condition (B3) is the same as the constraint equation (50), if $h_* = 0$. Kinetic boundary conditions with $\chi = 1$ corresponds to microscopically variational dynamics at thermodynamic equilibrium.

When $\chi = 0$, condition (B3) and the constraint equation (50) are equivalent if $h^0_* = \theta_{eq}(1 - M^0/D)$ and

$$\int d\eta \frac{1}{M^0} = 0. \tag{B7}$$

This relation implies a very strong constraint $\tilde{\nu}_+ = -\tilde{\nu}_-$, which is not expected in usual systems. In general, $\tilde{\nu}_+ \neq -\tilde{\nu}_-$, and the phase field model with $\chi = 0$ is not variational. (A noteworthy fact is that when $\tilde{\nu}_+ = -\tilde{\nu}_-$, the model with $\chi = 0$ is formally equivalent to the model with $\chi = 1$, where $\tilde{\beta}$ is simply corrected by a constant: $\tilde{\beta} \to \tilde{\beta} - \theta_{eq}/\tilde{\nu}_+$.)

2. Model with one concentration field per terrace

We here consider an isolated step. The generalization to an arbitrary number of steps is straightforward. We start with the energy functional

$$\begin{aligned} \mathcal{F}_2 = \int d\mathbf{x} \left[\frac{W^2}{2} (\nabla \phi)^2 + f + \frac{\lambda}{2\theta_{eq}\phi_+} (\theta_+ - \theta_{eq}\phi_+)^2 \right. \\ \left. + \frac{\lambda}{2\theta_{eq}\phi_-} (\theta_- - \theta_{eq}\phi_-)^2 \right]. \end{aligned} \tag{B8}$$

Following the same line as in the preceding section, we define

$$U_+ = h_+ + \theta_+, \tag{B9}$$

$$U_- = h_- + \theta_-. \tag{B10}$$

We now propose the relaxation model

$$\partial_t U_+ = \boldsymbol{\nabla}\left[M_+ \boldsymbol{\nabla} \left.\frac{\delta \mathcal{F}_2}{\delta U_+}\right|_{U_-,\phi}\right] - \mathcal{C}\left(\left.\frac{\delta \mathcal{F}_2}{\delta U_+}\right|_{U_-,\phi} - \left.\frac{\delta \mathcal{F}_2}{\delta U_-}\right|_{U_+,\phi}\right) - \frac{1}{\tau_e}\left.\frac{\delta \mathcal{F}_2}{\delta U_+}\right|_{U_-,\phi}, \tag{B11}$$

$$\partial_t U_- = \boldsymbol{\nabla}\left[M_- \boldsymbol{\nabla} \left.\frac{\delta \mathcal{F}_2}{\delta U_-}\right|_{U_+,\phi}\right] - \mathcal{C}\left(\left.\frac{\delta \mathcal{F}_2}{\delta U_-}\right|_{U_+,\phi} - \left.\frac{\delta \mathcal{F}_2}{\delta U_+}\right|_{U_-,\phi}\right) - \frac{1}{\tau_e}\left.\frac{\delta \mathcal{F}_2}{\delta U_-}\right|_{U_+,\phi}, \tag{B12}$$

$$\partial_t \phi = -\frac{1}{\tau_\phi}\left.\frac{\delta \mathcal{F}_2}{\delta \phi}\right|_{U_+,U_-}. \tag{B13}$$

This model decreases the energy functional $\mathcal{F}_2$. Indeed, up to negligible terms integrated along the boundary of the integration domain, one has

$$\begin{aligned}\frac{d}{dt}\mathcal{F}_2 &= \int d\mathbf{x}\left[\partial_t \phi \left.\frac{\delta \mathcal{F}_2}{\delta \phi}\right|_{U_+,U_-} + \partial_t U_+ \left.\frac{\delta \mathcal{F}_2}{\delta U_+}\right|_{U_-,\phi} + \partial_t U_- \left.\frac{\delta \mathcal{F}_2}{\delta U_-}\right|_{U_+,\phi}\right] \\ &= \int d\mathbf{x}\left[-\frac{1}{\tau_p}\left(\left.\frac{\delta \mathcal{F}_2}{\delta \phi}\right|_{U_+,U_-}\right)^2 - M_+\left(\boldsymbol{\nabla}\left.\frac{\delta \mathcal{F}_2}{\delta U_+}\right|_{\phi,U_-}\right)^2 - M_-\left(\boldsymbol{\nabla}\left.\frac{\delta \mathcal{F}_2}{\delta U_-}\right|_{\phi,U_+}\right)^2 - \mathcal{C}\left(\left.\frac{\delta \mathcal{F}_2}{\delta U_+}\right|_{\phi,U_-} - \left.\frac{\delta \mathcal{F}_2}{\delta U_-}\right|_{\phi,U_+}\right)^2 \right. \\ &\quad \left. - \frac{1}{\tau}\left(\left.\frac{\delta \mathcal{F}_2}{\delta U_+}\right|_{\phi,U_-}\right)^2 - \frac{1}{\tau_e}\left(\left.\frac{\delta \mathcal{F}_2}{\delta U_-}\right|_{\phi,U_+}\right)^2\right] \leqslant 0. \end{aligned} \tag{B14}$$

Defining

$$M_+ = \frac{\phi_+^2 \theta_{eq}}{\lambda}\mathcal{M}_+, \tag{B15}$$

$$M_- = \frac{\phi_-^2 \theta_{eq}}{\lambda}\mathcal{M}_-, \tag{B16}$$

$$\mathcal{C} = \frac{\theta_{eq}\phi_+\phi_-}{\lambda}\mathcal{B}, \tag{B17}$$

$$\tau_e = \lambda \tau, \tag{B18}$$

and neglecting second-order terms $\sim(\theta-\theta_{eq})^2$, the relaxation equations may be rewritten as

$$\partial_t \theta_+ + \partial_t h_+ = \boldsymbol{\nabla}[\mathcal{M}_+(\theta_+ \boldsymbol{\nabla}\phi_+ - \phi_+ \boldsymbol{\nabla}\theta_+)] - \mathcal{B}(\theta_+\phi_- - \theta_-\phi_+) - \frac{1}{\tau}(\theta_+ - \theta_{eq}\phi_+), \tag{B19}$$

$$\partial_t \theta_- + \partial_t h_- = \boldsymbol{\nabla}[\mathcal{M}_-(\theta_- \boldsymbol{\nabla}\phi_- - \phi_- \boldsymbol{\nabla}\theta_-)] - \mathcal{B}(\theta_-\phi_+ - \theta_+\phi_-) - \frac{1}{\tau}(\theta_- - \theta_{eq}\phi_-), \tag{B20}$$

$$\tau_\phi \partial_t \phi = W^2\nabla^2\phi - f_\phi + \lambda\left[(h_{+\phi} + \theta_{eq}\phi_{+\phi})\left(\frac{\theta_+}{\theta_{eq}\phi_+} - 1\right) + (h_{-\phi} + \theta_{eq}\phi_{-\phi})\left(\frac{\theta_-}{\theta_{eq}\phi_-} - 1\right)\right]. \tag{B21}$$

Comparing to the model in the main text Eqs. (73)–(75), we see that some conditions are needed for the phase field model to be variational at equilibrium (i.e., when $\theta_\pm^\infty = \theta_{eq}\phi_+$):

$$\mathcal{B}_{++} = \mathcal{B}_{-+} = \mathcal{B}\phi_-, \tag{B22}$$

$$\mathcal{B}_{-+} = \mathcal{B}_{--} = \mathcal{B}\phi_+, \tag{B23}$$

$$g_{+\phi}\theta_{eq}\phi_+ = h_{+\phi} + \theta_{eq}\phi_{+\phi}, \tag{B24}$$

$$g_{-\phi}\theta_{eq}\phi_- = h_{-\phi} + \theta_{eq}\phi_{-\phi}. \tag{B25}$$

Integrating and combining Eqs. (B24) and (B25), one finds

$$\frac{\int d\phi\, g_{+\phi}\phi_+}{\int d\phi(g_{+\phi}\phi_+ + g_{-\phi}\phi_-)} = \frac{[h_+]_-^+ - \theta_{eq}}{[h_+ + h_-]_-^+}, \tag{B26}$$

$$\frac{\int d\phi\, g_{-\phi}\phi_-}{\int d\phi(g_{+\phi}\phi_+ + g_{-\phi}\phi_-)} = \frac{[h_-]_-^+ + \theta_{eq}}{[h_+ + h_-]_-^+}. \tag{B27}$$

Combining Eqs. (93), (90), (94), and (99), we find that conditions (B26) and (B27) are verified only when $\chi = 1$. Therefore, the phase field model with $\chi = 1$ that verifies conditions (B22)–(B25) is variational at equilibrium. In contrast, for the model with $\chi = 0$ no variational formulation was found.

We will end this section with an example of functions $h_\pm$ and $g_\pm$ that obey conditions (B24)–(B25):

$$h_+ = -[\alpha(4\phi_+^3 - 3\phi_+^4) + \theta_{eq}\phi_+], \tag{B28}$$

$$h_- = -[-(1-\alpha)(4\phi_-^3 - 3\phi_-^4) + \theta_{eq}\phi_-], \tag{B29}$$

$$g_+ = (-3\phi_+^2 + 2\phi_+^3)2\alpha/\theta_{eq}, \tag{B30}$$

$$g_- = (3\phi_-^2 - 2\phi_-^3)2(1-\alpha)/\theta_{eq}. \tag{B31}$$

The four functions $h_\pm$ and $g_\pm$ are defined up to an arbitrary additive constant.

APPENDIX C: EXPLICIT MODELS WITH ONE CONCENTRATION FIELD

1. One step

Here, we want to consider one step only, the free energy f does not have to be periodic, and a simple double well potential is enough for our purpose

$$f = -\frac{\phi^2}{2} + \frac{\phi^4}{4}, \tag{C1}$$

$$g = \phi - \frac{2}{3}\phi^3 + \frac{\phi^5}{5}, \tag{C2}$$

$$\frac{D}{M} = 1 + m_s(1-\phi^2) + m_a\phi(1-\phi^2), \tag{C3}$$

and $h_* = 0$. The zeroth-order solution for ϕ is $\phi_0 = -\tanh(\eta/\sqrt{2})$. Using Eqs. (53) and (54), one finds

$$m_s = \frac{\tilde{d}_+ + \tilde{d}_-}{2W\sqrt{2}}, \tag{C4}$$

$$m_a = \frac{7}{6}\frac{\tilde{d}_+ - \tilde{d}_-}{W\sqrt{2}}, \tag{C5}$$

where $\tilde{d}_\pm = D/\tilde{\nu}_\pm$, and from Eqs. (56) and (57)

$$\lambda = \frac{5}{4\sqrt{2}}\frac{W}{\theta_{eq}^0\Gamma}, \tag{C6}$$

$$\frac{Da^*}{\lambda} = \frac{209}{525} + \frac{80}{231}m_s. \tag{C7}$$

2. A train of steps

A simple explicit model that has the required periodicity is

$$f = \frac{1}{\pi}\cos(\pi\phi), \tag{C8}$$

$$g = \phi + \frac{1}{\pi}\sin(\pi\phi), \tag{C9}$$

$$\frac{D}{M} = 1 + m_s[1+\cos(\pi\phi)] + m_a\sin(\pi\phi), \tag{C10}$$

with $h_* = 0$. Now, to zeroth order, ϕ is the solution of a sine-Gordon equation. Once again, Eqs. (53) and (54) lead to

$$m_s = \frac{\pi^{1/2}}{4}\frac{\tilde{d}_+ - \tilde{d}_-}{W}, \tag{C11}$$

$$m_a = \frac{3\pi^{3/2}}{32}\frac{\tilde{d}_+ - \tilde{d}_-}{W}, \tag{C12}$$

and with help of Eqs. (56) and (57)

$$\lambda = \frac{4}{\pi^{3/2}}\frac{W}{\theta_0^{eq}\Gamma}, \tag{C13}$$

$$\frac{Da^*}{\lambda} = 0.298\,235 + m_s\frac{64}{45\pi}. \tag{C14}$$

APPENDIX D: EXPLICIT MODELS WITH ONE CONCENTRATION FIELD PER TERRACE

1. Model A

A simple choice that satisfies Eqs. (92) and (89) is

$$\mathcal{B}_{++} = \mathcal{B}_{-+} = \mathcal{B}\phi_-, \tag{D1}$$

$$\mathcal{B}_{--} = \mathcal{B}_{+-} = \mathcal{B}\phi_+, \tag{D2}$$

with

$$W\int d\eta\,\mathcal{B}\phi_+^0\phi_-^0 = \nu. \tag{D3}$$

A specific choice that satisfies this relation is

$$\phi_+ + \phi_- = 1, \tag{D4}$$

$$\mathcal{B} = 6\nu|\nabla\phi_+| = 6\nu|\nabla\phi_-|. \tag{D5}$$

The first equation means that the total equilibrium concentration $\theta_{eq}\phi_+ + \theta_{eq}\phi_-$ to be strictly constant, even in the step region. We then define $h_\pm$ and $g_\pm$ as

$$h_+ = -(\alpha + \chi\theta_{eq})\phi_+, \tag{D6}$$

$$h_- = [1-(\alpha+\chi\theta_{eq})]\phi_-, \tag{D7}$$

$$g_+ = \alpha g, \tag{D8}$$

$$g_- = (1-\alpha)g. \tag{D9}$$

a. One step

For one step, the functions f and g can still be chosen as Eqs. (C1) and (C2). Then, we define

$$\phi_\pm = \frac{1}{2}(1 \mp \phi). \tag{D10}$$

Then, from Eq. (101)

$$\lambda = \frac{5}{2\sqrt{2}} \frac{1}{\theta^0_{eq}\Gamma}. \tag{D11}$$

b. A train of steps

For a train of steps, f and g are defined from Eqs. (C8) and (C9). For the three fields model, we then choose

$$\phi_\pm = \frac{1}{2}\left[1 \pm \sin\left(\frac{\pi}{2}\phi\right)\right]. \tag{D12}$$

We also define $z = \mathrm{sign}[\cos(\phi/2)]$. The terraces are then defined as the regions where $\phi = 2n+1$, where n is an integer. The value of the coupling constant is calculated using Eq. (101):

$$\lambda = \frac{8}{\pi^{3/2}} \frac{1}{\Gamma \theta^0_{eq}}. \tag{D13}$$

2. Model B

We now want to write down a model where the exchange term is simply proportional to the concentration difference $(\theta_+ - \theta_-)$. To do so, we still use Eqs. (D4) and (D6)–(D9), but

$$\mathcal{B}_{++} = \mathcal{B}_{-+} = 2\nu|\nabla\phi_+|, \tag{D14}$$

$$\mathcal{B}_{--} = \mathcal{B}_{+-} = 2\nu|\nabla\phi_-|, \tag{D15}$$

Conditions (92) and (89) are then fulfilled. The values of the coupling constant for one step or for a train of steps are still given by Eqs. (D11) and (D13), respectively.

APPENDIX E: STEP VELOCITY AND DISPERSION RELATION IN THE DISCONTINUOUS MODEL

We consider here the case $\chi = 0$. The calculation for the case $\chi = 1$ is similar. Moreover, an inspection of Eq. (18) shows that both cases lead to the same result when $\theta_{eq} \ll \chi(1-\chi)$.

Let us consider a perfect vicinal surface, i.e., all steps are separated by the same terrace width ℓ. During growth or sublimation, a steady state exist, where all steps have the same velocity, this is the step flow mode. We define

$$\frac{1}{\ell_d} = \frac{V}{D}, \quad x_s = (D\tau)^{1/2}, \quad \Delta = \Omega(\tau F - c^0_{eq}), \tag{E1}$$

and the length scales

$$\frac{1}{d} = \frac{\nu}{D} = \frac{1}{d_0} + \frac{1}{d_+ + d_-}, \tag{E2}$$

$$\delta = \beta D = (d_+^{-1} + d_-^{-1})^{-1}, \tag{E3}$$

$$x_d = \left(\frac{1}{4\ell_d^2} + \frac{1}{x_s^2}\right)^{-1}. \tag{E4}$$

We also define

$$s = \sinh(\ell/x_d), \quad c = \cosh(\ell/x_d), \tag{E5}$$

$$s_d = \sinh(\ell/2\ell_d), \quad c_d = \cosh(\ell/2\ell_d), \tag{E6}$$

and the determinant

$$\frac{\mathcal{D}_0}{2} = \frac{1}{\delta x_d}c + \frac{1}{\delta}\left(\frac{1}{d} + \frac{2\alpha - 1}{\ell_d}\right)s + \frac{2}{x_d d_0}(c - c_d). \tag{E7}$$

The steady state concentration on both sides of the step reads

$$\theta_{0+} - \theta_\infty = \frac{2}{\mathcal{D}_0}\left\{-\left(\frac{\alpha\Delta}{\delta} - \frac{\theta^\infty}{\ell_d}\right)\left[\left(\frac{1}{2\ell_d} + \frac{1-\alpha}{\delta} + \frac{1}{d_0}\right)s + \frac{1}{x_d}c\right] - \left(\frac{(1-\alpha)\Delta}{\delta} + \frac{\theta^\infty}{\ell_d}\right)\left[\frac{1}{x_d}e^{\ell/2\ell_d} + \frac{1}{d_0}s\right]\right\}, \tag{E8}$$

$$\theta_{0-} - \theta_\infty = \frac{2}{\mathcal{D}_0}\left\{-\left(\frac{(1-\alpha)\Delta}{\delta} + \frac{u_\infty}{\ell_d}\right)\left[\left(-\frac{1}{2\ell_d} + \frac{\alpha}{\delta} + \frac{1}{d_0}\right)s + \frac{1}{x_d}c\right] - \left(\frac{\alpha\Delta}{\delta} - \frac{u_\infty}{\ell_d}\right)\left[\frac{1}{x_d}e^{-\ell/2\ell_d} + \frac{1}{d_0}s\right]\right\}, \tag{E9}$$

where $\theta^\infty = \Omega\tau F$. An equation for the step velocity (or ℓ_d) is then obtained from mass conservation at the step

$$\mathcal{D}_0\frac{\delta}{2\ell_d} = \Delta\left\{\left[\left(\frac{1}{x_s^2} + \frac{1}{2\ell_d}\right)s - \frac{1}{x_d\ell_d}s_d\right] + \frac{2}{x_d d}(c - c_d)\right\} + \frac{\Omega c^0_{eq}}{\ell_d}\left\{\left(\frac{1}{2\ell_d}s - \frac{1}{x_d}s_d\right) + \frac{2\alpha - 1}{x_d}(c - c_d)\right\}. \tag{E10}$$

For small perturbations of the steps $\zeta_n(x,t)$, the discontinuous model is linearized. The Fourier transform of the perturbation ζ is defined as

$$\zeta_{\omega k\varphi} = \int dt \int dx \sum_n e^{-i(\omega t + kx + n\varphi)}\zeta_n(x,t). \tag{E11}$$

Going to Fourier space and using the discontinuous model to first order in ζ, a relation is found between ω, k, and φ. This is the dispersion relation

$$\frac{i\omega}{D}\frac{\mathcal{D}}{2}=-\left\{\frac{2\Lambda_d}{d}(p-p_d)+\Lambda^2 q\right\}\theta_{eq}^0\Gamma k^2+\left\{\left(\frac{i\omega}{D}+\frac{1}{x_s^2}\right)[(1-\alpha)\theta_{0+}+\alpha\theta_{0-}]-\frac{\Omega F}{D}-\frac{1}{d}(\partial_z\theta_{0+}-\partial_z\theta_{0-})\right\}\left[\frac{1}{2\ell_d}q-\Lambda_d q_d\right]$$
$$+\left\{\left(\frac{i\omega}{D}+\frac{1}{x_s^2}\right)[-(1-\alpha)\theta_{0+}+\alpha\theta_{0-}]-\frac{\Omega F}{D}(2\alpha-1)+\frac{1}{d}(\partial_z\theta_{0+}+\partial_z\theta_{0-})\right\}\Lambda_d[p-p_d]$$
$$+\left\{\left(\frac{i\omega}{D}+\frac{1}{x_s^2}\right)(\theta_{0+}-\theta_{0-})\left(\frac{1}{d}+\frac{2\alpha-1}{\ell_d}\right)+[\alpha\partial_z\theta_{0+}+(1-\alpha)\partial_z\theta_{0-}]\Lambda^2\right\}q+\left\{\left(\frac{i\omega}{D}+\frac{1}{x_s^2}\right)(\theta_{0+}-\theta_{0-})\right\}\Lambda_d p_d, \tag{E12}$$

where we have defined

$$\frac{\mathcal{D}}{2}=\Lambda_d p+\left(\frac{1}{d}+\delta\Lambda^2+\frac{2\alpha-1}{2\ell_d}\right)q+\frac{2\delta\Lambda_d}{d_0}(p-p_d), \tag{E13}$$

and

$$\Lambda=\left(\frac{i\omega}{D}+k^2+\frac{1}{x_s^2}\right)^{1/2}, \tag{E14}$$

$$\Lambda_d=\left(\frac{1}{4\ell_d^2}+\Lambda^2\right)^{1/2}, \tag{E15}$$

$$q=\sinh(\Lambda_d\ell), \tag{E16}$$

$$p=\cosh(\Lambda_d\ell), \tag{E17}$$

$$q_d=\sinh(i\varphi+\ell/2\ell_d), \tag{E18}$$

$$p_d=\cosh(i\varphi+\ell/2\ell_d), \tag{E19}$$

and the zeroth-order gradients at the steps are related to the concentration via

$$\partial_z\theta_{0+}=\alpha\frac{\theta_{0+}-\theta_{eq}}{\delta}+\frac{\theta_{0+}-\theta_{0-}}{d_0}-\frac{\theta_{0+}}{\ell_d}, \tag{E20}$$

$$\partial_z\theta_{0-}=-(1-\alpha)\frac{\theta_{0-}-\theta_{eq}}{\delta}+\frac{\theta_{0+}-\theta_{0-}}{d_0}-\frac{\theta_{0-}}{\ell_d}. \tag{E21}$$

Note that, although the notations are not well adapted to this case, the steady step velocity and the dispersion relation are perfectly well defined in the limit $\tau\to\infty$.

[1] W.K. Burton, N. Cabrera, and F.C. Frank, Philos. Trans. R. Soc. London, Ser. A **243**, 299 (1951); P. Nozières, in *Solids Far From Equilibrium* (Godrèche Alea-Saclay, Cambridge, 1992); A. Pimpinelli and J. Villain, *Physics of Crystal Growth* (Cambridge University Press, Cambridge, England, 1999).

[2] R.E. Caflisch, E. Weinan, M.F. Gyure, B. Merriman, and C. Ratsch, Phys. Rev. E **59**, 6879 (1999); O. Pierre-Louis, Phys. Rev. Lett. **87**, 106104 (2001); O. Pierre-Louis, M.R. D'Orsogna, and T.L. Einstein, *ibid.* **82**, 3661 (1999).

[3] I. Bena, C. Misbah, and A. Valance, Phys. Rev. B **47**, 7408 (1993).

[4] O. Pierre-Louis and C. Misbah, Phys. Rev. Lett. **76**, 4761 (1996); O. Pierre-Louis, C. Misbah, Y. Saito, J. Krug, and P. Politi, *ibid.* **80**, 4221 (1998).

[5] O. Pierre-Louis and T.L. Einstein, Phys. Rev. B **62**, 13 697 (2000).

[6] A. Karma and M. Plapp, Phys. Rev. Lett. **81**, 4444 (1998).

[7] F. Liu and H. Metiu, Phys. Rev. E **49**, 2601 (1997).

[8] O. Pierre-Louis and C. Misbah, Phys. Rev. B **58**, 2259 (1998).

[9] S. Tanaka, N.C. Bartelt, C.C. Umbach, R.M. Tromp, and J.M. Blakely, Phys. Rev. Lett. **78**, 3342 (1997).

[10] M. Ozdemir and A. Zangwill, Phys. Rev. B **45**, 3718 (1992).

[11] E. Ben-Jacob, N. Goldenfeld, J.S. Langer, and G. Schön, Phys. Rev. Lett. **51**, 1930 (1983).

[12] J.S. Langer and R.F. Sekerka, Acta Metall. **23**, 1225 (1975).

[13] G. Caginalp, Phys. Rev. A **39**, 5887 (1989).

[14] A. Karma and W.-J. Rappel, Phys. Rev. Lett. **77**, 4050 (1996); Phys. Rev. E **57**, 4323 (1998).

[15] G. Ehrlich and F.G. Hudda, J. Chem. Phys. **44**, 1039 (1966); J. Krug, P. Politi, and T. Michely, Phys. Rev. B **61**, 14037 (2000).

[16] E. Ben-Jacob, N. Goldenfeld, J.S. Langer, and G. Schön, Phys. Rev. Lett. **51**, 1930 (1983).

[17] O. Pierre-Louis, Surf. Sci. **529**, 114 (2003).

[18] A. Pimpinelli *et al.*, J. Phys.: Condens. Matter **6**, 2661 (1994).

[19] G.S. Bales and A. Zangwill, Phys. Rev. B **41**, 5500 (1990).

[20] R.J. Braun, G.B. McFadden, and S.R. Coriell, Phys. Rev. E **49**, 4336 (1994).

[21] J.-J. Métois and S. Stoyanov, Surf. Sci. **440**, 407 (1999).

[22] A. Saúl, J.-J. Métois, and A. Ranguis, Phys. Rev. B **65**, 075409 (2002).

[23] A. Karma, Phys. Rev. Lett. **87**, 115701 (2001).